OVA, Cat-OVAs or poly-L-lysine (PLL), the assay was conducted.

2.7. In vivo disposition experiment

OVA and Cat-OVAs were radiolabeled with ^{111}In using the bifunctional chelating agent DTPA anhydride according to the method of Hnatowich et al. [21]. ^{111}In-labeled antigen proteins were subcutaneously injected into the footpad of male ddY mice at a dose of 50 μl per mouse in 2 mg/ml protein solution. At appropriate times after administration, under ether anesthesia, leg (injection site), the liver, kidney and spleen were isolated, rinsed with saline and weighed. Plasma was obtained from the blood by centrifugation. The amount of ^{111}In radioactivity in urine was also determined by collecting the urine remaining in the bladder. The radioactivity in each sample was counted in a well-type NaI-scintillation counter (ARC-500, Aloka, Tokyo, Japan).

2.8. CTL assay

C57BL/6 mice were immunized four times at weekly interval in the footpad with OVA, Cat-OVAs or OVA emulsified in Freund's complete adjuvant (CFA) [22] at a dose of 50 μl per mouse in 2 mg/ml protein solution. Ten days after the last immunization, splenocytes were isolated from the immunized mice and restimulated in vitro for 5 days with mitomycin C-treated E.G7. Target cells (E.G7 or EL4; EL4 was used as a target control) were labeled with ^{51}Cr by incubating with $Na_2{}^{51}CrO_4$ in culture medium for 45 min at 37 °C. After washing, 2×10^4 of ^{51}Cr-labeled target cells and serially diluted splenocytes were coincubated in 200 μl culture medium for 4 h at 37 °C. Spontaneous release of ^{51}Cr with no effector cells and maximal release in the presence of 1% NP40 were also evaluated. Cells were centrifuged (1500 rpm) for 5 min, and 100 μl of each supernatant was collected for radioactivity measurements. The cytolytic activity of CTLs was calculated as [23]:

$$\%\ \text{killing} = 100 \times \left\{ \frac{\text{observed release} - \text{spontaneous release}}{\text{maximal release} - \text{spontaneous release}} \right\}.$$

2.9. Tumor challenge experiment

C57BL/6 mice were immunized twice at weekly intervals in the footpad with each antigen. Eight days after the last immunization, 1×10^6 per mouse of E.G7 were administered intradermally into the back as a challenge. The tumor size was measured with a slide caliper and expressed as a tumor index, determined as the square root of (major axis × minor axis). The survival time of the tumor-challenged mice was also recorded.

2.10. Assessment of local damage at the injection site

ddY mice were immunized subcutaneously in the footpad with OVA, Cat_9-OVA, Cat_{20}-OVA, OVA/cationic liposome complexes, or OVA emulsified in CFA. OVA/cationic liposome complexes were prepared as follows: cationic liposomes (DOTMA:DOPE = 1:1) were mixed at a final concentration of 1.85 mg/ml with OVA dissolved in 5% dextrose and incubated for more than 30 min at RT [24,25]. After 24 h, the footpad thickness was measured with a micro-meter and the degree of footpad swelling was calculated by subtracting the mean thickness of the footpad of mice which were injected with no antigen.

3. Results

3.1. In vitro cellular association of Cat-OVAs with antigen-presenting cells

We initially examined the cellular association of Cat-OVAs with DC2.4 cells in comparison with native OVA using FITC-labeled proteins. Confocal microscopic studies demonstrated that, after a 1 h incubation at 37 °C, the fluorescence derived from OVA was observed in a punctate pattern in the cells (Fig. 1A), indicating that OVA was probably internalized by endocytosis by the DCs. On the other hand, much stronger fluorescent signals were observed in

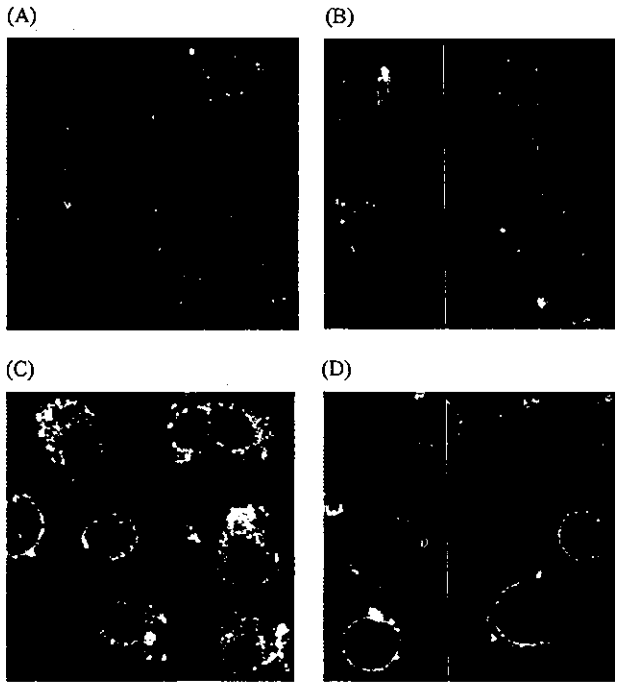

Fig. 1. Cellular association of FITC-labeled OVA and Cat-OVAs with DC2.4 cells. DC2.4 cells were incubated with 1 mg/ml FITC-labeled OVA or 200 μg/ml FITC-labeled Cat-OVAs for 1 h at 37 or 4 °C. The nuclei were stained with propidium iodide. (A) OVA at 37 °C; (B) Cat_9-OVA at 37 °C; (C) Cat_{20}-OVA at 37 °C; (D) Cat_{20}-OVA at 4 °C.

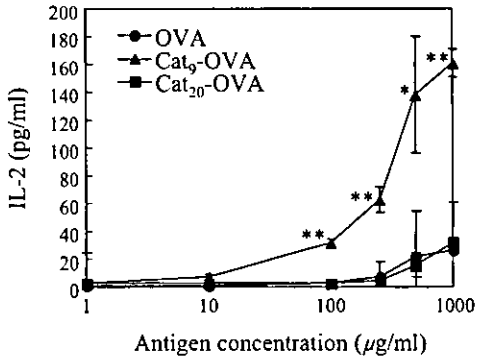

Fig. 2. MHC class I presentation of native OVA and Cat-OVAs by DC2.4 cells. DC2.4 cells (5×10^4 per well) were incubated with various concentrations of antigen and CD8OVA1.3 T hybridoma cells (1×10^5 per well) at 37 °C. After 24 h, IL-2 production from CD8OVA1.3 T hybridoma cells was measured by ELISA. Results are expressed as the mean ± S.D. (●) OVA; (▲) Cat_9-OVA; (■) Cat_{20}-OVA. $^*P < 0.05$ or $^{**}P < 0.01$ compared with the OVA group.

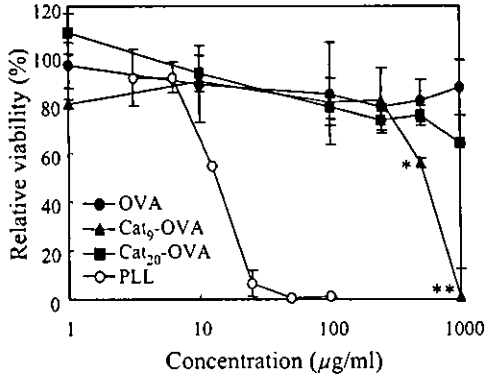

Fig. 3. Effect of native OVA, Cat-OVAs and poly-L-lysine (PLL) on DC2.4 cell viability measured by MTT assay after 24-h incubation at 37 °C. Results are expressed as the mean ± S.D. (●) OVA; (▲) Cat_9-OVA; (■) Cat_{20}-OVA. $^*P < 0.05$ or $^{**}P < 0.01$ compared with the OVA group.

the cells treated with FITC-labeled Cat-OVAs, although the applied concentration of Cat-OVAs was as little as one-fifth compared with that of OVA (Fig. 1B and C). In particular, Cat_{20}-OVA exhibited a marked cellular uptake. The fluorescence derived from Cat_{20}-OVA was also localized in the cytoplasm, suggesting that part of the internalized Cat_{20}-OVA was transferred into the cytoplasm. At 4 °C, only binding at the cellular surface was observed (Fig. 1D). These images confirm that Cat-OVAs are efficiently taken up by DC2.4 through adsorptive endocytosis based on electrostatic interaction.

3.2. MHC class I presentation and cytotoxicity

In order to examine whether Cat-OVAs are presented on MHC class I following cellular uptake, we conducted an antigen presentation assay (Fig. 2). In the case of native OVA, a slight IL-2 induction was observed at a higher concentration. In contrast, Cat_9-OVA exhibited a high level of presentation on MHC class I, suggesting that this OVA derivative has a potential to increase the immune response. However, Cat_{20}-OVA was scarcely presented under these experimental conditions in spite of extensive uptake by DC2.4 cells, indicating that further cationization was less effective to the class I peptide presentation in this system.

We also examined the cytotoxicity of OVA and Cat-OVAs against DC2.4 by MTT assay because polycations such as poly-L-lysine have cytotoxicity [26,27]. OVA and Cat_9-OVA did not show any significant cytotoxicity against the DCs, although cellular damage was observed at higher concentrations of Cat_{20}-OVA (Fig. 3). Marked cytotoxicity was observed for poly-L-lysine under the same conditions.

3.3. Augmentation of in vivo immune response by cationization

Prior to in vivo evaluation, we examined the biodisposition of native OVA and Cat-OVAs after subcutaneous injection into the footpad. Native OVA and Cat_9-OVA gradually disappeared from the injection site and distributed to

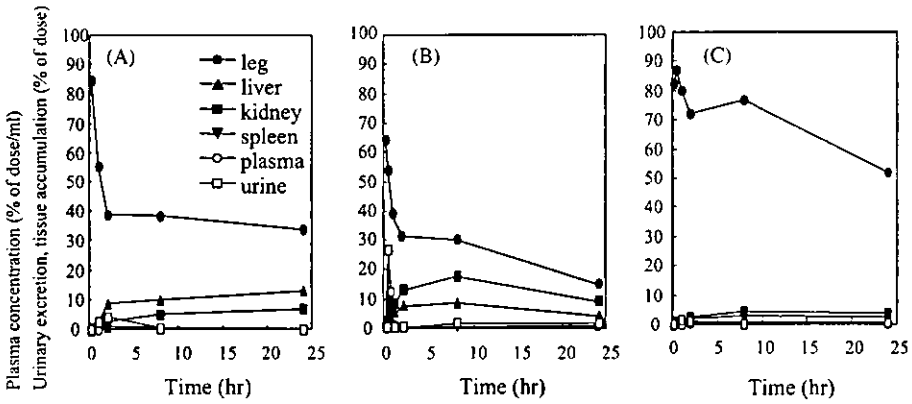

Fig. 4. Time-course of plasma concentrations, tissue accumulation and urinary excretion of native OVA (A), Cat_9-OVA (B) and Cat_{20}-OVA (C) after subcutaneous injection in mice at a dose of 100 μg per mouse. Results are expressed as the mean ± S.D. (●) Leg (injection site); (▲) liver; (■) kidney; (▼) spleen; (○) plasma; (□) urine.

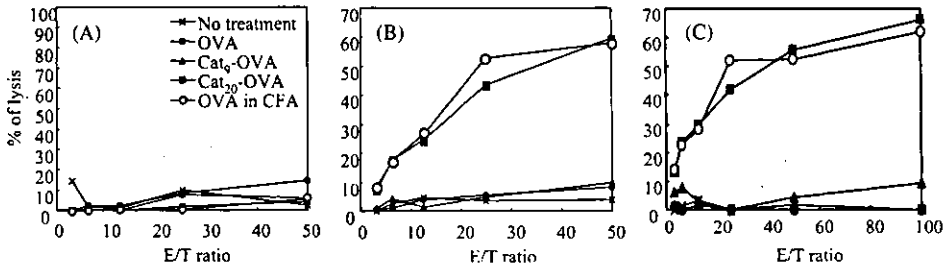

Fig. 5. Induction of OVA-specific CTLs by immunization with native OVA, Cat-OVAs and OVA in CFA. Mice were immunized four times with 100 μg OVA or Cat-OVAs and 10 days after the last immunization, splenocytes were isolated and ^{51}Cr release assay was performed after 5 days. E.G7 (A) and EL4 (B) were used as the target cells and specific lysis (C) was calculated by subtracting the % killing of EL4 from that of E.G7. (×) No treatment; (●) OVA; (▲) Cat_9-OVA; (■) Cat_{20}-OVA; (○) OVA in CFA.

various organs (Fig. 4A and B). In contrast, elimination of Cat_{20}-OVA from the injection site was very slow and more than 50% of it remained there with restricted distribution to organs (Fig. 4C).

To evaluate whether antigen-specific CTLs were elicited by subcutaneous immunization with soluble antigens, native OVA or Cat-OVAs, we examined the OVA-specific CTL response using E.G7 cells expressing OVA (Fig. 5). The splenocytes from the mice immunized with unmodified OVA showed no significant induction of OVA-specific CTLs. A slight CTL induction was observed in the group of Cat_9-OVA immunization. The splenocytes from Cat_{20}-OVA-treated mice showed a very high level of OVA-specific CTL activity comparable with that from the mice treated with OVA in CFA, which has a stronger immune stimulating activity than any other adjuvants, although it produces severe toxicity.

We also examined the ability of Cat-OVA immunaization to provide a protective effect in vivo against an E.G7 tumor challenge. A significant inhibitory effect on tumor growth was observed in Cat_{20}-OVA-immunized mice (Fig. 6). Native OVA and Cat_9-OVA had marginal effect. OVA in CFA displayed the most significant effect. Similar results were

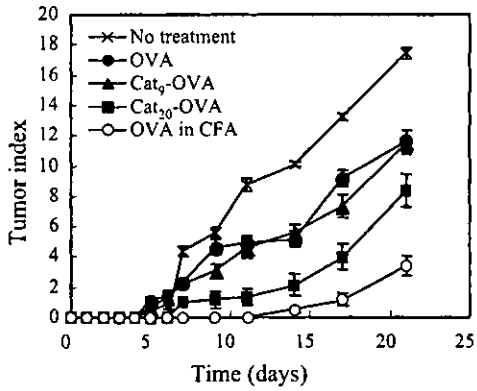

Fig. 6. In vivo growth inhibitory effect produced by immunization with native OVA, Cat-OVAs and OVA in CFA. Mice were immunized twice and 7 days after the last immunization, 1×10^6 cells of E.G7 were challenged intradermally. (×) No treatment; (●) OVA; (▲) Cat_9-OVA; (■) Cat_{20}-OVA; (○) OVA in CFA. Results are expressed as the mean ± S.E.M.

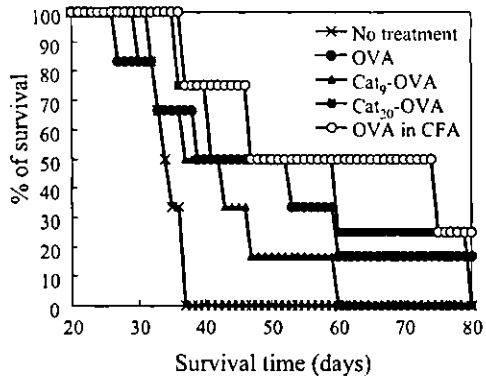

Fig. 7. Prolongation of survival time by immunization with native OVA, Cat-OVAs and OVA in CFA. Mice were immunized twice and 7 days after the last immunization, 1×10^6 cells of E.G7 were challenged intradermally. (×) No treatment; (●) OVA; (▲) Cat_9-OVA; (■) Cat_{20}-OVA; (○) OVA in CFA.

obtained for the survival of mice challenged with E.G7 tumor cells (Fig. 7, Table 2).

3.4. Tissue damage after local injection

In order to assess the local tissue damage at the injection sites, we compared the footpad swelling at 24 h after immunization (Fig. 8). A cationic liposome formulation was also tested because there are several reports claiming that the immune response is potentiated by antigens used with cationic liposomes [24,25,28–30]. Subcutaneous injection of native OVA did not induce any swelling at the injection site. As expected, marked footpad swelling was observed in OVA

Table 2
Mean survival time of immunized mice on tumor challenge

Antigen	Mean survival time
No treatment	33.7 ± 0.843
OVA	41.4 ± 6.16
Cat_9-OVA	40.7 ± 4.47
Cat_{20}-OVA	53.3 ± 10.02[a]
OVA in CFA	57.3 ± 10.5[a]

[a] Significantly prolonged compared to the no treatment group.

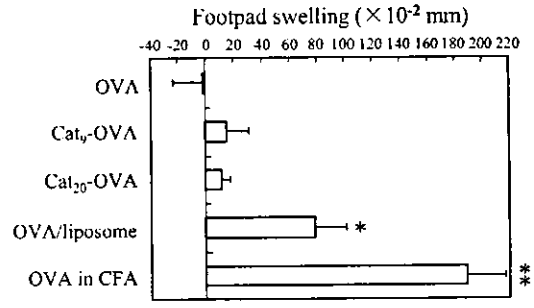

Fig. 8. Footpad swelling in mice immunized with OVA, Cat-OVAs, OVA/liposome complexes or OVA in CFA. Mice were immunized with 100 μg OVA, Cat-OVAs, OVA/liposome complexes or OVA in CFA and 24 h after immunization, the footpad swelling was measured. Results are expressed as mean ± S.D. $^*P < 0.05$ or $^*P < 0.01$ compared with the OVA group.

in CFA-treated mice, probably due to local inflammation. OVA/cationic liposome complexes also induced significant footpad swelling. On the other hand, no significant swelling was observed in mice challenged with Cat-OVAs, suggesting that the soluble cationic proteins did not induce any local damage at the injection sites.

4. Discussion

In the present study, we demonstrate, for the first time, that antigen-specific CTLs can be effectively elicited by cationization of a soluble antigen protein without any adjuvants. We have evaluated the ability of two kinds of Cat-OVAs with different cationic charges to elicit a CTL response through enhanced uptake by APCs and concomitant participation in the class I pathway. Cat_{20}-OVA, a cationized OVA derivative with more cationic charges, showed a pronounced induction of the OVA-specific CTL response after subcutaneous immunization. The CTL response was comparable with that induced by OVA with CFA, which is the strongest adjuvant although it has severe toxic effects. In contrast to the CFA formulation that actually produced local tissue damage in this study, Cat_{20}-OVA appeared to be safer. Cat_{20}-OVA also showed a significant protective effect on the growth of OVA-expressing E.G7 tumor cells, although the effect of OVA with CFA was superior to that of Cat_{20}-OVA.

However, contrary to our expectation that both Cat-OVAs showed a higher class I presentation compared with native OVA due to enhanced cellular uptake by DC2.4 cells, in vitro experiments demonstrated that Cat_{20}-OVA failed to show an efficient class I presentation whereas Cat_9-OVA showed a high level of class I presentation in the DC2.4/CD8OVA1.3 system. For the antigen presentation, fragmentation of the antigen and binding of the fragmented antigen to the class I molecule would be necessary. CD8OVA1.3 recognizes only SIINFEKL, one of the OVA class I epitope. Probably, not all but some-OVA epitopes are acylated by the cationization process since it contains glutamic acid, a target amino acid of cationization. Although Cat-OVAs should undergo appropriate processing to generate the epitope for class I presentation after endocytic uptake by DC2.4 cells, acylation of the epitope would affect the processing in the DCs. This effect might be significant in the case of Cat_{20}-OVA with a higher degree of chemical modification and enhanced uptake by DC2.4 cells did not result in efficient class I presentation. Even if the acylated epitope was successfully presented on the class I, CD8OVA1.3 might not recognize the epitope. It has been reported that alteration of epitopes could even cause an antagonistic effect in antigen recognition via T cell receptors [31] and the glutamic acid in this epitope may be involved in recognition via T cell receptors [32]. In addition, cytotoxicity of Cat_{20}-OVA against DC2.4 cells at the higher concentration may be involved in the results of the antigen presentation assay. In the case of Cat_9-OVA, the effect of epitope modification would be less likely, accounting for the fact that this derivative exhibited a high presentation efficacy of the epitope in the assay. Enhanced cellular uptake of Cat_9-OVA by DC2.4 cells would significantly contribute to this result. On the other hand, high level of cytolytic activity against OVA-expressing E.G7 tumor cells was observed in vivo by immunization with Cat_{20}-OVA while that against EL4 was low level. This result suggests that immunization with Cat_{20}-OVA elicited antigen-specific response in which OVA-specific CTLs should involved, although we did not clarify the MHC restriction of the cytolytic activity. Non-specific cytotoxic effect mediated by NK cells, $CD4^+$ T cells and macrophages might be also involved in the result, but it should not be significant according to the low level of cytolytic activity against EL4. Therefore, antigen presentation may occur in a different way from that under in vitro conditions. After subcutaneous immunization, APCs, residing in the skin including Langerhans cells, would play an important role in Cat-OVA uptake, processing and subsequent antigen presentation. Our pharmacokinetic study suggests that Cat_{20}-OVA should have an advantage over Cat_9-OVA and native OVA in terms of efficient uptake by APCs in the skin since Cat_{20}-OVA showed a prolonged retention at the injection site, which will significantly increase the availability for the target cells. The processing of Cat-OVA in these APCs may be different from that by DC2.4 cells. The acylated epitope in Cat_{20}-OVA might be properly processed to generate the typical epitope, SIINFEKL, and presented on MHC class I. In addition, some epitopes other than SIINFEKL, presented on MHC class I not having glutamic acid nor asparaginic acid, both of which are targets of cationization, might be also involved in recognition by T cells.

Although previous studies have also demonstrated an increased immune response using cationized antigen proteins, CTL induction was not reported. Michael and co-workers reported that the cationized form of BSA showed enhanced immunogenicity in an animal model [10,33–35]. Farmer et al. demonstrated that cationized diphtheria toxoid was an effective inducer of human antigen-specific T cell response [11,36]. In these studies, the enhanced immune response by

cationized antigen proteins was due to enhancement of antigen uptake by APCs and subsequent stimulation of helper T cells. We also speculated that, after immunization with Cat_{20}-OVA, efficient antigen presentation on MHC class II should occur as well as on class I and both CTLs and helper T cells should be activated. It is possible that cytotoxic $CD4^+$ T cells [37], macrophage-mediated tumor cytotoxicity and antibody-mediated cellular cytotoxicity [38], as well as $CD8^+$ CTL, were involved in protective effect on the growth of tumor cells. It has been reported that $CD4^+$ CTL clones are capable of killing tumor cells such as melanoma by perforin/granzyme pathway of Fas/FasL interaction and that activated macrophages are able to recognize and lyse tumor cells by the release of cytotoxic mediators including TNF-α, IL-1, nitric oxide and reactive oxygen intermediates or phagocytosis. Otherwise, it is also possible that $CD8^+$ CTL activation takes place in a $CD4^+$ T cells independent manner because Cat_{20}-OVA was avidly taken up by APCs [39]. This phenomenon may have contributed to the prolonged survival of tumor-challenged mice, since the responsiveness of $CD4^+$ T cells has been reported to be reduced in the tumor-bearing state [40].

In the case of Cat_{20}-OVA immunization, we anticipated local tissue damage at the injection site because cytotoxicity of Cat_{20}-OVA was observed in vitro at the higher concentration (Fig. 3). However, Cat_{20}-OVA as well as Cat_9-OVA showed no significant local tissue damage in vivo whereas OVA/liposome complex showed local tissue damage (Fig. 8). It was likely that the local concentration of Cat_{20}-OVA did not reach to a cytotoxic level presumably due to diffusion of the soluble cationic protein at the injection site following subcutaneous administration. The strategy of cationization has been exploited for the purpose of efficiently delivering a variety of proteins, and either cationic polymers or cationic liposomes are commonly utilized for gene delivery [41]. In particular, it has been reported that cationic liposomal delivery of OVA is a useful strategy for inducing an OVA-specific CTL response [28,29]. The result of assessment of local damage suggests that Cat-OVAs would be safer than the cationic liposome formulation tested in this study.

In conclusion, this is the first demonstration that a high level of CTL activity could be achieved by immunization with a water-soluble cationized antigen without any adjuvants. Moreover, no major local tissue damage by this vaccine was observed. These findings have important implications for the future design of protein- or peptide-based vaccines.

References

[1] Germain RN, Margulies DH. The biochemistry and cell biology of antigen processing and presentation. Annu Rev Immunol 1993;11:403.

[2] Harding CV, Song R. Phagocytic processing of exogenous particulate antigens by macrophages for presentation by class I MHC molecules. J Immunol 1994;153:4925.

[3] Shen Z, Reznikoff G, Dranoff G, Rock KL. Cloned dendritic cells can present exogenous antigens on both MHC class I and class II molecules. J Immunol 1997;158:2723.

[4] Norbury CC, Chambers BJ, Prescott AR, Ljunggren HG, Watts C. Constitutive macropinocytosis allows TAP-dependent major histocompatibility complex class I presentation of exogenous soluble antigen by bone marrow-derived dendritic cells. Eur J Immunol 1997;27:280.

[5] Rodriguez A, Regnault A, Kleijmeer M, Ricciardi-Castagnoli P, Amigorena S. Selective transport of internalized antigens to the cytosol for MHC class I presentation in dendritic cells. Nat Cell Biol 1999;1:362.

[6] Regnault A, Lankar D, Lacabanne V, Rodriguez A, Thery C, Rescigno M, et al. Fcgamma receptor-mediated induction of dendritic cell maturation and major histocompatibility complex class I-restricted antigen presentation after immune complex internalization. J Exp Med 1999;189:371.

[7] Bansal P, Mukherjee P, Basu SK, George A, Bal V, Rath S. MHC class I-restricted presentation of maleylated protein binding to scavenger receptors. J Immunol 1999;162:4430.

[8] Mitchell DA, Nair SK, Gilboa E. Dendritic cell/macrophage precursors capture exogenous antigen for MHC class I presentation by dendritic cells. Eur J Immunol 1998;28:1923.

[9] Banchereau J, Steinman RM. Dendritic cells and the control of immunity. Nature 1998;392:245.

[10] Apple RJ, Domen PL, Muckerheide A, Michael JG. Cationization of protein antigens. IV. Increased antigen uptake by antigen-presenting cells. J Immunol 1988;140:3290.

[11] Farmer JL, Roberts LA, Rydzinski ME, Hilty MD. Human immune response to cationized proteins. II. Characterization of interaction of cationized diphtheria toxoid with human mononuclear cells. Cell Immunol 1993;146:198.

[12] Hong G, Chappey O, Niel E, Scherrmann JM. Enhanced cellular uptake and transport of polyclonal immunoglobulin G and fab after their cationization. J Drug Target 2000;8:67.

[13] Futami J, Maeda T, Kitazoe M, Nukui E, Tada H, Seno M, et al. Preparation of potent cytotoxic ribonucleases by cationization: enhanced cellular uptake and decreased interaction with ribonuclease inhibitor by chemical modification of carboxyl groups. Biochemistry 2001;40:7518.

[14] Nishikawa M, Hasegawa S, Yamashita F, Takakura Y, Hashida M. Electrical charge on protein regulates its absorption from the rat small intestine. Am J Physiol Gastrointest Liver Physiol 2002;282:G711.

[15] Pfeifer JD, Wick MJ, Roberts RL, Findlay K, Normark SJ, Harding CV. Phagocytic processing of bacterial antigens for class I MHC presentation to T cells. Nature 1993;361:359.

[16] Moore MW, Carbone FR, Bevan MJ. Introduction of soluble protein into the class I pathway of antigen processing and presentation. Cell 1988;54:777.

[17] Habeeb AF. Determination of free amino groups in proteins by trinitrobenzenesulfonic acid. Anal Biochem 1966;14:328.

[18] Monsigny M, Roche AC, Midoux P. Uptake of neoglycoproteins via membrane lectin(s) of L1210 cells evidenced by quantitative flow cytofluorometry and drug targeting. Biol Cell 1984;51:187.

[19] Nakanishi K, Watanabe Y, Maruyama M, Yamashita F, Takakura Y, Hashida M. Secretion polarity of interferon-beta in epithelial cell lines. Arch Biochem Biophys 2002;402:201.

[20] Supino R. MTT assays. Methods Mol Biol 1995;43:137.

[21] Hnatowich DJ, Layne WW, Childs RL. The preparation and labeling of DTPA-coupled albumin. Int J Appl Radiat Isot 1982;33:327.

[22] Ke Y, Li Y, Kapp JA. Ovalbumin injected with complete Freund's adjuvant stimulates cytolytic responses. Eur J Immunol 1995;25:549.

[23] Collins DS, Findlay K, Harding CV. Processing of exogenous liposome-encapsulated antigens in vivo generates class I MHC-restricted T cell responses. J Immunol 1992;148:3336.

[24] Okada N, Tsujino M, Hagiwara Y, Tada A, Tamura Y, Mori K, et al. Administration route-dependent vaccine efficiency of murine dendritic cells pulsed with antigens. Br J Cancer 2001;84:1564.

[25] Okada N, Saito T, Mori K, Masunaga Y, Fujii Y, Fujita J, et al. Effects of lipofectin-antigen complexes on major histocompatibility complex class I-restricted antigen presentation pathway in murine dendritic cells and on dendritic cell maturation. Biochim Biophys Acta 2001;1527:97.
[26] Choksakulnimitr S, Masuda S, Tokuda H, Takakura Y, Hashida M. In vitro cytotoxicity of macromolecules in different cell culture systems. J Control Release 1995;34:233.
[27] Fischer D, Li Y, Ahlemeyer B, Krieglstein J, Kissel T. In vitro cytotoxicity testing of polycations: influence of polymer structure on cell viability and hemolysis. Biomaterials 2003;24:1121.
[28] Nakanishi T, Kunisawa J, Hayashi A, Tsutsumi Y, Kubo K, Nakagawa S, et al. Positively charged liposome functions as an efficient immunoadjuvant in inducing immune responses to soluble proteins. Biochem Biophys Res Commun 1997;240:793.
[29] Nakanishi T, Kunisawa J, Hayashi A, Tsutsumi Y, Kubo K, Nakagawa S, et al. Positively charged liposome functions as an efficient immunoadjuvant in inducing cell-mediated immune response to soluble proteins. J Control Release 1999;61:233.
[30] Chikh G, Schutze-Redelmeier MP. Liposomal delivery of CTL epitopes to dendritic cells. Biosci Rep 2002;22:339.
[31] Jameson SC, Carbone FR, Bevan MJ. Clone-specific T cell receptor antagonists of major histocompatibility complex class I-restricted cytotoxic T cells. J Exp Med 1993;177:1541.
[32] Jameson SC, Bevan MJ. Dissection of major histocompatibility complex (MHC) and T cell receptor contact residues in a Kb-restricted ovalbumin peptide and an assessment of the predictive power of MHC-binding motifs. Eur J Immunol 1992;22:2663.
[33] Muckerheide A, Apple RJ, Pesce AJ, Michael JG. Cationization of protein antigens. I. Alteration of immunogenic properties. J Immunol 1987;138:833.
[34] Muckerheide A, Domen PL, Michael JG. Cationization of protein antigens. II. Alteration of regulatory properties. J Immunol 1987;138:2800.
[35] Domen PL, Muckerheide A, Michael JG. Cationization of protein antigens. III. Abrogation of oral tolerance. J Immunol 1987;139:3195.
[36] Farmer JL, Roberts LA, Rydzinski ME, Hilty MD. Human immune response to cationized proteins. I. Characterization of the in vitro response to cationized diphtheria toxoid. Cell Immunol 1993;146:186.
[37] Hahn S, Gehri R, Erb P. Mechanism and biological significance of CD4-mediated cytotoxicity. Immunol Rev 1995;146:57.
[38] Klimp AH, de Vries EG, Scherphof GL, Daemen T. A potential role of macrophage activation in the treatment of cancer. Crit Rev Oncol Hematol 2002;44:143.
[39] Rock KL, Clark K. Analysis of the role of MHC class II presentation in the stimulation of cytotoxic T lymphocytes by antigens targeted into the exogenous antigen-MHC class I presentation pathway. J Immunol 1996;156:3721.
[40] Zou JP, Shimizu J, Ikegame K, Yamamoto N, Ono S, Fujiwara H, Hamaoka T. Tumor-bearing mice exhibit a progressive increase in tumor antigen-presenting cell function and a reciprocal decrease in tumor antigen-responsive CD4+ T cell activity. J Immunol 1992;148:648.
[41] Blau S, Jubeh TT, Haupt SM, Rubinstein A. Drug targeting by surface cationization. Crit Rev Ther Drug Carrier Syst 2000;17:425.

Immunology 2004 **112** 211–218 doi:10.1111/j.1365-2567.2004.01871.x

Efficient scavenger receptor-mediated uptake and cross-presentation of negatively charged soluble antigens by dendritic cells

KOHSUKE SHAKUSHIRO, YASUOMI YAMASAKI, MAKIYA NISHIKAWA & YOSHINOBU TAKAKURA
Department of Biopharmaceutics and Drug Metabolism, Graduate School of Pharmaceutical Sciences, Kyoto University, Kyoto, Japan

SUMMARY

Exogenous antigens endocytosed in large amounts by antigen-presenting cells (APC) are presented on major histocompatibility complex (MHC) class I molecules as well as on class II molecules, a process called cross-presentation. Among APC, dendritic cells (DC) play a key role in cross-presentation by transporting internalized antigen to the cytosol. The present study shows that ovalbumin (OVA) introduced with negative charges by succinylation (Suc-OVA), maleylation (Mal-OVA) or *cis*-aconitylation (Aco-OVA) was efficiently taken up by DC via scavenger receptors (SR). Mal-OVA and Aco-OVA were efficiently cross-presented by DC, while cross-presentation of Suc-OVA was hardly observed. MHC class I presentation of acylated OVA introduced directly into the cytosol was inefficient and presentation of exogenous native OVA but not of Aco-OVA was markedly augmented by chloroquine, an inhibitor of endosomal acidification, suggesting that deacylation in endosomes or lysosomes is necessary for cross-presentation of acylated OVA. MHC class I presentation of exogenous native OVA and Aco-OVA by DC was blocked by lactacystin and brefeldin A, demonstrating that exogenous antigens taken up by DC are cross-presented through the conventional cytosolic pathway. Therefore, SR-mediated delivery of antigen to DC leads to efficient cross-presentation, although the pathway of chemical modification should be considered.

Keywords dendritic cells: cross-presentation, MHC class I presentation, scavenger receptors; soluble antigens: negatively charged, ovalbumin

INRODUCTION

Successful immunotherapy against cancer or infectious diseases requires induction of cytotoxic T lymphocyte (CTL)-mediated immune responses. Antigen-specific CTL are generated when antigen-presenting cells (APC) present peptides from antigen on major histocompatibility complex (MHC) class I molecules to naïve $CD8^+$ T cells. In general, however, proteins taken up by APC are degraded in endosomal/lysosomal compartments and presented on MHC class II molecules, while MHC class I molecules associate exclusively with peptides derived from endogenously synthesized proteins, such as virus-encoded proteins or tumour antigen.[1] Therefore, it is not expected that exogenous antigen gain access to the MHC class I antigen presentation pathway and initiate CTL responses.

However, APC are able to present exogenous antigens on MHC class I molecules under certain conditions, a process called cross-presentation.[2,3] Although macrophages and B cells are capable of cross-presentation *in vitro*,[4–6] dendritic cells (DC) are most likely to be crucial in this process because of their distinctive ability to prime naïve T cells and generate CTL responses *in vivo*.[7] In addition to phagocytosis[4,8] and macropinocytosis,[9,10] antigen endocytosed via Fcγ receptors[11] and scavenger receptors (SR)[5,12–14] are efficiently cross-presented to $CD8^+$ T cells by APC.

SR, which recognize diverse polyanionic ligands,[15] are expressed on macrophages, B cells and DC, and negatively charged proteins obtained by succinylation or maleylation

Received 17 September 2003; revised 20 January 2004; accepted 12 March 2004.

Abbreviations: DC, dendritic cell; SR, scavenger receptor.

Correspondence: Dr Y. Takakura, Department of Biopharmaceutics and Drug Metabolism, Graduate School of Pharmaceutical Sciences, Kyoto University, Sakyo-ku, Kyoto 606-8501, Japan. E-mail: takakura@pharm.kyoto-u.ac.jp

are known to be SR ligands.[16,17] Thus, using such chemical modifications, antigens are expected to be efficiently taken up by APC through SR-mediated endocytosis.

In this study, in order to investigate the possibility that efficient cross-presentation of soluble antigens by DC can be achieved through SR-mediated delivery and to study its mechanism, ovalbumin (OVA), which was selected as a model antigen, was introduced with negatively charges obtained via three forms of acylation, namely, succinylation (Suc-OVA), maleylation (Mal-OVA) and *cis*-aconitylation (Aco-OVA). Cellular uptake and subsequent MHC class I presentation of these chemically modified OVA were studied using a well-characterized DC line, DC2.4.[18,19]

MATERIALS AND METHODS

Chemicals

OVA, fluorescein isothiocyanate (FITC), polyinosinic acid (poly[I]), polycytidylic acid (poly[C]), bovine serum albumin (BSA), lactacystin, brefeldin A and chloroquine were purchased from Sigma (St. Louis, MO). Succinic anhydride was purchased from Nacalai Tesque (Kyoto, Japan). Maleic anhydride and *cis*-aconitic anhydride were purchased from Wako Pure Chemical Industries (Osaka, Japan). Diethylenetriaminepentaacetic acid (DTPA) anhydride was purchased from Dojindo Laboratory (Kumamoto, Japan). The $OVA_{257-264}$ peptide, SIINFEKL was purchased from Bachem (Bubendorf, Switzerland). $^{111}InCl_3$ was supplied by Nihon Medi-Physics (Takarazuka, Japan). All other chemicals were reagent-grade products obtained commercially.

Cell lines

The murine DC line DC2.4 (haplotype H-2^b) was a generous gift from Dr K. L. Rock (University of Massachusetts Medical Center, Worcester, MA).[18] DC2.4 cells display dendritic morphology, express a series of DC-specific markers, MHC class I and II molecules, costimulatory molecules, and have phagocytic property and antigen-presenting capacity.[18] CD8OVA1.3 T hybridoma cells, which secrete IL-2 upon stimulation with SIINFEKL-K^b complexes,[20] were kindly provided by Dr C. V. Harding (Case Western Reserve University, Cleveland, OH).

DC2.4 cells were cultured in RPMI-1640 medium (Nissui Pharmaceutical, Tokyo, Japan) supplemented with 10% fetal bovine serum (Equitech-Bio, Kerrville, TX), 50 μM 2-mercaptoethanol, 2 mM L-glutamine, and antibiotics (all from Invitrogen, Carlsbad, CA). CD8OVA1.3 cells were grown in Dulbecco's modified Eagle medium (Nissui) supplemented as described for RPMI-1640 medium.

Chemical modification of OVA

OVA was modified with succinic, maleic or *cis*-aconitic anhydride (Aco-OVA) at alkaline pH.[16,21,22] In brief, OVA was dissolved in 0·2 M Tris buffer (pH 8·65), and an appropriate amount of each anhydride was added to the solution. The mixture was stirred until all the anhydride dissolved and kept at pH > 8 during the reaction. After the reaction was complete, free anhydride was removed by gel filtration with a Sephadex G-25 column (Amersham Biosciences, Piscataway, NJ). The protein fractions were then concentrated by ultrafiltration, and finally lyophilized. The purity of these products was confirmed by isoelectric focusing and unmodified OVA was not detected in all the derivatives. Thus, the products were used in following experiments without further purifications. The degree of modification was assessed by estimating the loss of free amino groups as measured by trinitrobenzenesulphonic acid (TNBS).[23]

Evaluation of deacylation of acylated OVA by hydrolysis

Each acylated OVA was dissolved in phosphate-buffered saline at pH 5·0 or 7·4, and incubated at 37°. At appropriate intervals, aliquots were collected and free amino groups were determined using TNBS. Deacylation at each time point was evaluated as the ratio of the remaining acylated amino groups.

Confocal microscopy

OVA, Suc-OVA and Aco-OVA were labelled with FITC by the method of Monsigny *et al.*[24] DC2.4 cells cultured on glass coverslips were incubated with FITC-labelled proteins at 37°. After 6 hr, cells were washed and fixed with 4% paraformaldehyde. Confocal images were observed with a laser scanning confocal microscope (MRC-1024, Bio-Rad, Hercules, CA).

Cellular association experiments

For cellular association experiments, proteins were radiolabelled with ^{111}In using the bifunctional chelating agent DTPA anhydride according to the method of Hnatowich *et al.*[25] This radiolabeling method is suitable for the study of cellular association because any radioactive metabolites produced after cellular uptake are retained within the cells.[26] DC2.4 cells cultured on 24-well plates were added to Hanks' balanced salt solution (HBSS) containing indicated concentrations of ^{111}In-labelled proteins and incubated at 37°. After indicated times, the protein solution was removed and cells were washed with ice-cold HBSS. Cells were then solubilized with 0·3 N NaOH with 0·1% Triton-X-100 and the radioactivity in the cell lysate was measured using a well-type NaI-scintillation counter (ARC-500, Aloka, Tokyo, Japan). The amount of cellular protein in each cell lysate was estimated using a protein quantification kit (Dojindo Laboratory).

In competition experiments, ^{111}In-labelled Suc-OVA was added to DC2.4 cells concomitantly with a variety of unlabelled macromolecules.

Antigen-presentation assays

Various concentrations of antigen were added to DC2.4 cells (5×10^4/well) cultured on 96-well plates and incubated with CD8OVA1.3 T hybridoma cells (10^5/well) at 37°. After 24 hr, the cell culture supernatants were collected and freeze–thawed. Then, the response of CD8OVA1.3 T cells was determined by measuring interleukin-2 (IL-2) levels in the supernatants with enzyme-linked immunosorbent assay

(ELISA; AN'ALYZA mouse IL-2, Genzyme-Techne, Minneapolis, MN). The antigen presentation experiments were carried out in the presence of serum to maintain normal cellular functions of DC2.4 and CD8OVA1.3 T cells during the experiments. Although serum might contain SR ligands including lipoproteins that may affect the antigen uptake, the effect of these putative ligands would be negligible since the antigen concentration was high (up to 1–5 mg/ml).

In some assays, antigen was introduced directly into the cytosol by osmotic lysis of pinosomes.[27] Briefly, each antigen was dissolved in hypertonic medium (RPMI-1640 medium containing 0·5 M sucrose, 10% polyethylene glycol 1000 and 10 mM HEPES) at 5 mg/ml. DC2.4 cells were pelleted and resuspended at 2×10^6/ml in antigen-containing hypertonic medium for 10 min at 37°. The suspension was diluted to 30-fold with hypotonic medium (60% RPMI-1640 and 40% water) and left for 2–3 min at 37°. Cells were then pelleted, resuspended in culture medium and plated at different cell numbers. After a 3-hr incubation at 37°, cells were fixed with 1% paraformaldehyde and incubated with CD8OVA1.3 T hybridoma cells (10^5/well) for 20 hr. IL-2 levels in the culture supernatants were determined by ELISA.

To study the pathway for antigen presentation, DC2.4 cells (10^5/well) were incubated with 100 μM chloroquine, 10 μM lactacystin, or 5 μg/ml brefeldin A for 30 min prior to the addition of antigen. Cells were further incubated for 6 hr at 37° in the continued presence of inhibitor, washed and fixed. Then CD8OVA1.3 T hybridoma cells (10^5/well) were added and, after 20 hr, the IL-2 levels in the supernatants were measured.

RESULTS

Chemical modification of OVA

As shown in Table 1, the 18·3, 19·1, and 14·8 amino groups of OVA were modified with succinic (Suc-OVA), maleic (Mal-OVA) and *cis*-aconitic anhydride (Aco-OVA), respectively. These three derivatives seemed to possess enough negative charges to have an affinity for SR.[28]

Deacylation of acylated OVA by hydrolysis

In the recognition of antigenic peptide presented on MHC molecules, T cells strictly discriminate the structure of the peptide using T-cell receptors (TCR). Accordingly, the acyl group on the antigenic peptide may affect the TCR recognition. It has been demonstrated that maleyl and *cis*-aconityl groups introduced into proteins are removed by hydrolysis at an acidic pH, unlike succinyl groups.[29] Thus, deacylation of each acylated OVA by hydrolysis was investigated at pH 7·4 and 5·0, assuming physiological and endosomal/lysosomal conditions, respectively. At pH 5·0, the acyl groups of Aco-OVA were removed by hydrolysis in a time-dependent manner ($t_{1/2}$ = 3·97 hours) (Fig. 1a). Mal-OVA also underwent hydrolysis, although the rate was slower than Aco-OVA ($t_{1/2}$ = 78·8 hr). On the other hand, deacylation of Suc-OVA was hardly observed under these conditions. All three derivatives were stable at pH 7·4 (Fig. 1b). These results suggest that after being endocytosed, Aco-OVA and Mal-OVA are deacylated in acidic compartments such as endosomes and lysosomes and returned to native OVA, whereas they are stable in the extracellular fluid.

Table 1. Characteristics of acylated OVA*

Compound	Number of modified amino groups	Number of free amino groups	Estimated molecular weight
OVA	0	21	46 000
Suc-OVA	18·3	2·7	47 800
Mal-OVA	19·1	1·9	47 900
Aco-OVA	14·8	6·2	48 300

*The numbers and molecular weights were estimated using TNBS.

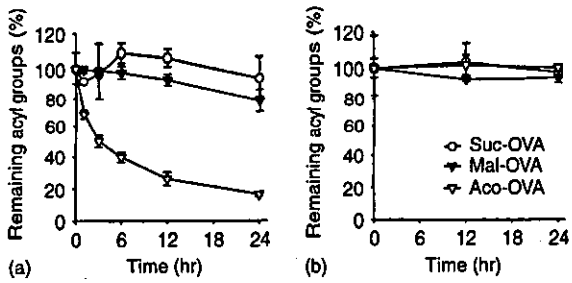

Figure 1. Deacylation of acylated OVA under acidic or neutral conditions. Acylated OVA in phosphate buffered saline pH 5·0 (a) or 7·4 (b) was incubated for the indicated times at 37°. The ratio of remaining acyl groups on each protein was determined by estimating the number of acylated amino groups at each time point using TNBS. Results are expressed as the mean ± SD (n = 3).

Internalization of acylated OVA into endocytic compartments

Figure 2 shows confocal microscopic images of uptake of FITC-labelled native and acylated OVA by DC2.4 cells. Punctate vesicular staining by FITC-labelled proteins was observed within DC2.4 cells, suggesting that after binding to the DC, acylated OVA was internalized into endocytic compartments.

Cellular association experiments

All the ^{111}In-labelled proteins were taken up by DC2.4 cells in a time- and concentration-dependent manner, and acylated OVA were more efficiently taken up by DC2.4 cells than native OVA (Fig. 3). Because the association of each protein was saturable and its amount was higher in acylated OVA than in native OVA which is taken up through mannose receptors,[30] it is likely that other receptors, probably SR also participate in the uptake of acylated OVA.

To study the uptake mechanism of acylated OVA, competition experiments were performed using ^{111}In-labelled

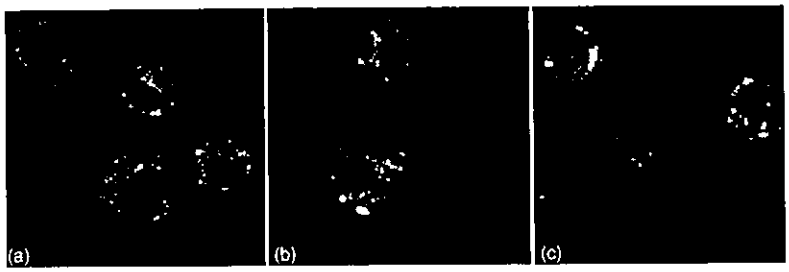

Figure 2. Intracellular localization of FITC-labelled native OVA (a), Suc-OVA (b), and Aco-OVA (c) in DC2.4 cells. DC2.4 cells were incubated with 1 mg/ml FITC-labelled proteins for 6 hr at 37°.

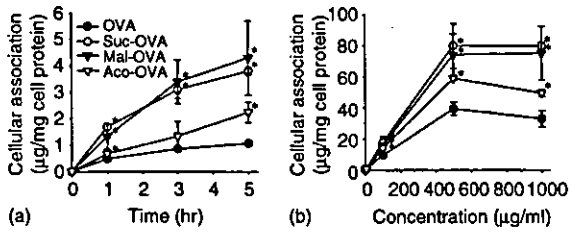

Figure 3. Time-course and concentration–dependence of cellular association of ^{111}In-labelled native or acylated OVA in DC2.4 cells. DC2.4 cells were incubated with ^{111}In-labelled proteins at 5 μg/ml for indicated times (a) or at various concentrations for 3 hr (b) at 37°. Results are expressed as the mean ± SD ($n = 3$). $^*P < 0.05$ versus OVA by Student's t-test.

Suc-OVA and excess amounts of unlabelled native or acylated OVA, maleylated BSA (Mal-BSA), poly[I], or poly[C]. The amount of cellular association of ^{111}In-Suc-OVA with DC2.4 cells was significantly reduced by all kinds of unlabelled acylated OVA (Fig. 4). Furthermore, poly[I] and Mal-BSA, but not poly[C], inhibited the cellular association of ^{111}In-Suc-OVA. These results demonstrate that each acylated OVA is endocytosed by DC via the same receptors, that is, SR.

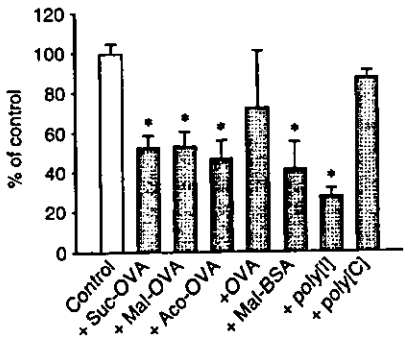

Figure 4. Inhibition of cellular association of ^{111}In-labelled Suc-OVA with DC2.4 cells. ^{111}In-Suc-OVA (10 μg/ml) was added to DC2.4 cells concomitantly with unlabelled protein (500 μg/ml), poly[I] or poly[C] (100 μg/ml) and incubated for 3 hr at 37°. Results are expressed as the mean ± SD ($n = 3$). $^*P < 0.01$ versus control by Student's t-test.

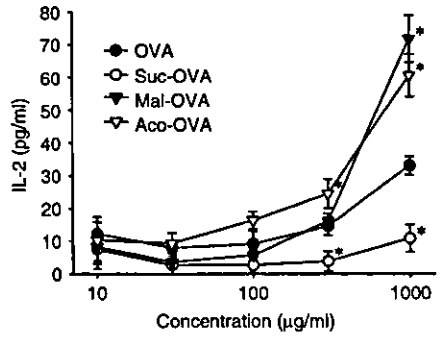

Figure 5. MHC class I presentation of exogenous native or acylated OVA by DC2.4 cells. DC2.4 cells (5×10^4/well) were incubated with various concentrations of antigen and CD8OVA1.3 T hybridoma cells (10^5/well) at 37°. After 24 hr, IL-2 production from CD8OVA1.3 T hybridoma cells was measured by ELISA. Results are expressed as the mean ± SD ($n = 3$). $^*P < 0.05$ versus OVA by Student's t-test.

Cross-presentation of native and acylated OVA

Figure 5 shows MHC class I presentation of exogenous native and acylated OVA by DC2.4 cells. Aco-OVA and Mal-OVA, which showed enhanced uptake by DC2.4 cells and deacylation under acidic conditions, were efficiently cross-presented to CD8OVA1.3 T hybridoma cells. In contrast, despite the higher association with DC2.4 cells, Suc-OVA induced a lower response of CD8OVA1.3 cells than native OVA.

The most prominent difference between Suc-OVA and Aco-OVA or Mal-OVA seems to be the chemical stability under acidic conditions (Fig. 1). Therefore, to ascertain whether deacylation in endosomes or lysosomes is essential for MHC class I presentation, each antigen was delivered directly into the cytosol of DC2.4 cells, and the response of CD8OVA1.3 T cells to the antigen-introduced DC2.4 cells was examined. When cytosolically delivered, Aco-OVA and Mal-OVA failed to generate a higher response of CD8OVA1.3 cells than native OVA (Fig. 6). Furthermore, the effects of endosomal acidification on MHC class I presentation of exogenous native OVA and Aco-OVA was also studied using chloroquine, which raises the pH in the endosomal/lysosomal compartments. Treatment with

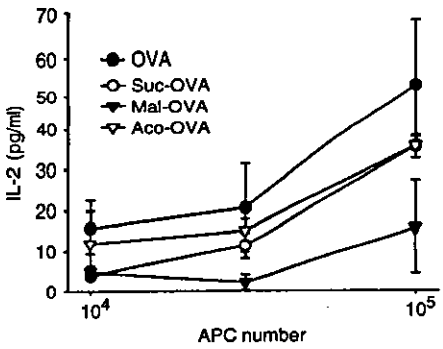

Figure 6. MHC class I presentation of osmotically introduced native or acylated OVA in DC2.4 cells. Each antigen (5 mg/ml) was introduced directly into the cytosol of DC2.4 cells by osmotic lysis of pinosomes. After a 3-hr incubation at 37°, cells were fixed, further incubated with CD8OVA1.3 T hybridoma cells (10^5/well) for 20 hr, and the levels of IL-2 in the supernatants were determined by ELISA. Results are expressed as the mean ± SD ($n = 3$).

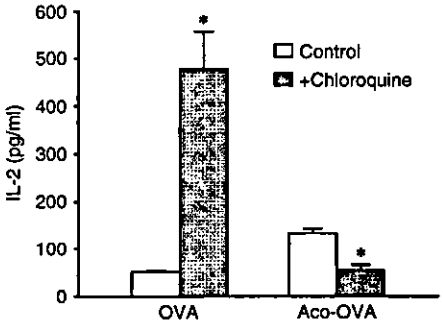

Figure 7. Effects of chloroquine on MHC class I presentation of exogenous antigen by DC2.4 cells. DC2.4 cells (10^5/well) were incubated with or without chloroquine (100 μM) for 30 min at 37° and mixed with 3 mg/ml native OVA or Aco-OVA. After a 6-hr chase in the continued presence of chloroquine, cells were washed, fixed and incubated with CD8OVA1.3 T hybridoma cells (10^5/well) for 20 hr. IL-2 levels in the culture supernatants were determined by ELISA. Results are expressed as the mean ± SD ($n = 3$). *$P < 0.005$ versus control by Student's t-test.

chloroquine dramatically enhanced the MHC class I presentation of exogenous native OVA, while the presentation of Aco-OVA was reduced (Fig. 7). Taken together, these results indicate that acyl groups on lysine residues in OVA prevent processing for MHC class I presentation by DC and/or recognition of antigenic peptide SIINFEKL by T cells. Consequently, exogenous Suc-OVA failed to elicit the response of CD8OVA1.3 T cells, whereas Aco-OVA and Mal-OVA were efficiently presented because of their reversibility at acidic pH.

The results in Fig. 7 also suggest that after endocytosis of exogenous antigens, peptides to be presented on MHC class I molecules are generated outside the endosomal/lysosomal compartments in DC. Endogenous cytosolic proteins are primarily degraded into peptides by proteasomes. The peptides are then transported into the

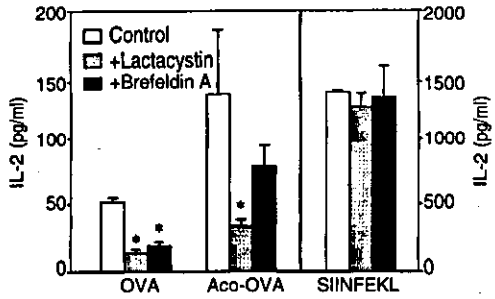

Figure 8. Effects of lactacystin and brefeldin A on MHC class I presentation of exogenous antigens by DC2.4 cells. DC2.4 cells (10^5/well) were incubated with or without lactacystin (10 μM) or brefeldin A (5 μg/ml) for 30 min at 37° and mixed with 3 mg/ml native OVA, Aco-OVA or 0·1 μg/ml SIINFEKL. After a 6-hr chase in the continued presence of inhibitors, cells were washed, fixed and incubated with CD8OVA1.3 T hybridoma cells (10^5/well) for 20 hr. IL-2 levels in the culture supernatants were determined by ELISA. Results are expressed as the mean ± SD ($n = 3$). *$P < 0.05$ versus control by Student's t-test.

endoplasmic reticulum (ER) by transporters associated with antigen processing (TAP), where they bind to nascent MHC class I molecules. The newly assembled peptide-MHC complexes are transported to the cell surface and presented to $CD8^+$ T cells.[31] To examine whether exogenous native and acylated OVA is cross-presented by DC via this pathway, the effects of lactacystin, a proteasome inhibitor, and brefeldin A, an inhibitor of anterograde ER-Golgi transport were examined. Both lactacystin and brefeldin A blocked MHC class I presentation of exogenous native OVA and Aco-OVA but not of SIINFEKL, which does not require intracellular processing for presentation (Fig. 8). These results indicate that exogenous native and acylated OVA are transported to the cytosol from endosomes or lysosomes and processed via the conventional MHC class I presentation pathway.

DISCUSSION

It is well-known that cross-presentation occurs when APC take up a large amount of exogenous antigens by phagocytosis,[4,8] macropinocytosis,[9,10] or receptor-mediated endocytosis.[5,11–14,32] APC express a variety of endocytic receptors, such as mannose receptors,[33] Fcγ receptors,[11,34] and SR.[5,12–14]

Among APC, DC are considered to be responsible for *in vivo* cross-presentation. It has been demonstrated that DC are the only type of APC that efficiently transport exogenous antigens to the cytosol.[35] Therefore, specific receptor-mediated antigen delivery to DC can be a promising approach for the development of effective vaccines.

In the present study, OVA was introduced with negative charges for the purpose of efficient SR-mediated uptake and cross-presentation by DC. Three kinds of negatively charged OVA, Suc-OVA, Mal-OVA, and Aco-OVA were synthesized and evaluated with respect to cellular association and cross-presentation.

Acylated OVA was efficiently taken up by DC2.4 cells compared with native OVA (Fig. 3), and the uptake was mediated by SR (Fig. 4). SR family has been divided into six classes[15] and most SR can bind a variety of anionic macromolecules, including modified low density lipoproteins (LDL), polynucleotides, and negatively charged proteins. It has been reported that SR are involved in the cross-presentation of antigen from apoptotic (CD36)[12] and live (SR-A)[14] cells by DC and that of maleylated antigen by macrophages and B cells.[5] Moreover, SR-, especially lectin-like oxidized LDL receptor-1 (LOX-1)-mediated uptake and cross-presentation of heat-shock protein-antigen conjugates by DC has been recently reported,[13] thereby supporting the usefulness of SR-mediated antigen delivery to DC. In this study, which SR are expressed on the surface of DC2.4 cells and involved in the uptake of acylated OVA was not examined in detail although it is of particular interest. The distinct, but partly overlapping, binding properties of the SR classes represent a complication in defining their respective activity in terms of ligand uptake. Therefore, the biological response after the recognition of acylated OVA might be unpredictable. However, this approach can also be efficacious in *in vivo* vaccination, since OVA-specific CTL were efficiently induced after subcutaneous injection of acylated OVA in mice (Yamasaki *et al.* manuscript in preparation). We speculated that LOX-1 might be involved in the uptake of acylated OVA because the inhibition profile shown (Fig. 4) was consistent with that of LOX-1.[13] In fact, expression of LOX-1 on the surface of DC2.4 cells was confirmed by immunostaining (data not shown). However, the details remain to be elucidated.

After SR-mediated endocytosis by DC2.4 cells, enhanced presentation of antigenic peptides SIINFEKL on MHC class I molecules to CD8OVA1.3 T hybridoma cells was observed in the case of Mal-OVA and Aco-OVA, while presentation of Suc-OVA was inefficient (Fig. 5). Native and acylated OVA taken up by DC were accumulated in endocytic compartments (Fig. 2), and under acidic conditions, maleyl and *cis*-aconityl, but not succinyl groups on lysine residues in OVA were removed by hydrolysis (Fig. 1a). Thus, it appears that deacylation of Mal-OVA and Aco-OVA occurs in endosomes or lysosomes and that Suc-OVA remains unhydrolysed in such compartments. Reduced presentation of Suc-OVA is thought to be attributed to this chemical stability in the acidic compartments. Direct introduction of acylated OVA into the cytosol resulted in a lower response of CD8OVA1.3 T cells than that of native OVA (Fig. 6), supporting this speculation.

The speculation was further confirmed using chloroquine, an inhibitor of endosomal acidification. MHC class I presentation of exogenous native OVA by DC2.4 cells was markedly augmented by chloroquine treatment and the level of MHC class I presentation of Aco-OVA was reduced by this drug (Fig. 7), probably as a consequence of suppression of deacylation in the acidic compartments. It is conceivable that enhanced cross-presentation of native OVA was caused by the inhibitory effect of chloroquine on proteolysis by cathepsins, which require an acidic environment for activity. This finding also indicates that proteolysis of OVA in the endosomal/lysosomal compartments is not required for the cross-presentation by DC and that the processing takes place in the cytosol. Rather, endocytic degradation is likely to abrogate the cross-presentation. Chloroquine has been reported to slightly enhance MHC class I presentation of exogenous bead-conjugated OVA by DC2.4 cells,[18] although the data on native OVA were not available. The difference in sensitivity to chloroquine between native and bead-conjugated OVA can be explained by the difference in size, because transport of internalized antigen to the cytosol within DC is size-selective.[35]

The cytosolic pathway for cross-presentation of native and acylated OVA within DC was examined using lactacystin, a proteasome inhibitor, and brefeldin A, an inhibitor of anterograde ER-Golgi transport. MHC class I presentation of exogenous native OVA and Aco-OVA by DC2.4 cells was inhibited by both drugs (Fig. 8), suggesting that internalized antigen in the endosomal/lysosomal compartments are delivered to the cytosol and presented on MHC class I molecules via the conventional pathway. It has been reported that in cross-presentation of Mal-OVA by macrophages, processing takes place in endosomes or lysosomes, not in the cytosol.[5] These two results probably reflect the type of APC used in each study, because antigen transport to the cytosol is restricted to DC[35] and the endosomal MHC class I presentation pathway is exclusively involved in the case of macrophages.[8,20]

In summary, exogenous Mal-OVA and Aco-OVA are efficiently taken up by DC via SR, deacylated in endosomes or lysosomes and transferred to the cytosol. The deacylated Mal-OVA and Aco-OVA in the cytosol are then processed via the conventional cytosolic pathway, which results in enhanced MHC class I presentation. Although DC also efficiently take up Suc-OVA by SR-mediated endocytosis, conceivably the succinyl groups on lysine residues are not removed since Suc-OVA is chemically stable under acidic conditions. As a result, even if transported to the cytosol, Suc-OVA induces a poor response of CD8OVA1.3 T-cell hybridomas. Possible reasons for this are that succinyl groups inhibit ubiquitin conjugation on lysine residues which is thought to be important in proteasomal degradation[36] and that succinylated SIINFEKL cannot be recognized by CD8OVA1.3 cells through TCR, since lysine residue on SIINFEKL is important for TCR recognition.[37,38]

In conclusion, the present study reveals that efficient cross-presentation can be achieved by antigen delivery to DC by chemical modification. In applications involving various types of tumour antigen, *cis*-aconitylation might be superior to maleylation, because *cis*-aconitylation can introduce two minus charges per amino group and therefore it can give antigen an affinity for SR with less modification than maleylation.[39] These findings should provide useful information for optimizing the design of *in vivo* cancer immunotherapy strategies based on the targeting of antigens in a soluble form to DC.

ACKNOWLEDGMENTS

We thank Dr Kenneth L. Rock (University of Massachusetts Medical Center, Worcester, MA) for providing DC2·4 cells and Dr Clifford V. Harding (Case Western Reserve University, Cleveland, OH) for providing CD8OVA1.3 T hybridoma cells.

This work was supported in part by a Grant-in-Aid for Scientific Research from the Ministry of Education, Culture, Sports, Science and Technology of Japan.

REFERENCES

1 Germain RN, Margulies DH. The biochemistry and cell biology of antigen processing and presentation. Annu Rev Immunol 1993; **11**:403–50.

2 Yewdell JW, Norbury CC, Bennink JR. Mechanisms of exogenous antigen presentation by MHC class I molecules in vitro and in vivo. implications for generating $CD8^+$ T cell responses to infectious agents, tumors, transplants, and vaccines. Adv Immunol 1999; **73**:1–77.

3 Heath WR, Carbone FR. Cross-presentation, dendritic cells, tolerance and immunity. Annu Rev Immunol 2001; **19**:47–64.

4 Kovacsovics-Bankowski M, Clark K, Benacerraf B, Rock KL. Efficient major histocompatibility complex class I presentation of exogenous antigen upon phagocytosis by macrophages. Proc Natl Acad Sci U S A 1993; **90**:4942–6.

5 Bansal P, Mukherjee P, Basu SK, George A, Bal V, Rath S. MHC class I-restricted presentation of maleylated protein binding to scavenger receptors. J Immunol 1999; **162**:4430–7.

6 Ke Y, Kapp JA. Exogenous antigens gain access to the major histocompatibility complex class I processing pathway in B cells by receptor-mediated uptake. J Exp Med 1996; **184**:1179–84.

7 Banchereau J, Steinman RM. Dendritic cells and the control of immunity. Nature 1998; **392**:245–52.

8 Harding CV, Song R. Phagocytic processing of exogenous particulate antigens by macrophages for presentation by class I MHC molecules. J Immunol 1994; **153**:4925–33.

9 Norbury CC, Hewlett LJ, Prescott AR, Shastri N, Watts C. Class I MHC presentation of exogenous soluble antigen via macropinocytosis in bone marrow macrophages. Immunity 1995; **3**:783–91.

10 Norbury CC, Chambers BJ, Prescott AR, Ljunggren HG, Watts C. Constitutive macropinocytosis allows TAP-dependent major histocompatibility complex class I presentation of exogenous soluble antigen by bone marrow-derived dendritic cells. Eur J Immunol 1997; **27**:280–8.

11 Regnault A, Lankar D, Lacabanne V *et al.* Fcgamma receptor-mediated induction of dendritic cell maturation and major histocompatibility complex class I-restricted antigen presentation after immune complex internalization. J Exp Med 1999; **189**:371–80.

12 Albert ML, Pearce SF, Francisco LM, Sauter B, Roy P, Silverstein RL, Bhardwaj N. Immature dendritic cells phagocytose apoptotic cells via alphavbeta5 and CD36, and cross-present antigens to cytotoxic T lymphocytes. J Exp Med 1998; **188**:1359–68.

13 Delneste Y, Magistrelli G, Gauchat J *et al.* Involvement of LOX-1 in dendritic cell-mediated antigen cross-presentation. Immunity 2002; **17**:353–62.

14 Harshyne LA, Zimmer MI, Watkins SC, Barratt-Boyes SM. A role for class A scavenger receptor in dendritic cell nibbling from live cells. J Immunol 2003; **170**:2302–9.

15 Terpstra V, van Amersfoort ES, van Velzen AG, Kuiper J, van Berkel TJ. Hepatic and extrahepatic scavenger receptors: function in relation to disease. Arterioscler Thromb Vasc Biol 2000; **20**:1860–72.

16 Takakura Y, Fujita T, Furitsu H, Nishikawa M, Sezaki H, Hashida M. Pharmacokinetics of succinylated proteins and dextran sulfate in mice: Implications for hepatic targeting of protein drugs by direct succinylation via scavenger receptors. Int J Pharm 1994; **105**:19–29.

17 Haberland ME, Fogelman AM. Scavenger receptor-mediated recognition of maleyl bovine plasma albumin and the demaleylated protein in human monocyte macrophages. Proc Natl Acad Sci USA 1985; **82**:2693–7.

18 Shen Z, Reznikoff G, Dranoff G, Rock KL. Cloned dendritic cells can present exogenous antigens on both MHC class I and class II molecules. J Immunol 1997; **158**:2723–30.

19 Okada N, Saito T, Mori K *et al.* Effects of lipofectin-antigen complexes on major histocompatibility complex class I-restricted antigen presentation pathway in murine dendritic cells and on dendritic cell maturation. Biochim Biophys Acta 2001; **1527**:97–101.

20 Pfeifer JD, Wick MJ, Roberts RL, Findlay K, Normark SJ, Harding CV. Phagocytic processing of bacterial antigens for class I MHC presentation to T cells. Nature 1993; **361**:359–62.

21 Butler PJG, Hartley BS. Maleylaion of amino groups. Methods Enzymol 1972; **25**:191–9.

22 Schoen P, Corver J, Meijer DK, Wilschut J, Swart PJ. Inhibition of influenza virus fusion by polyanionic proteins. Biochem Pharmacol 1997; **53**:995–1003.

23 Habeeb AF. Determination of free amino groups in proteins by trinitrobenzenesulfonic acid. Anal Biochem 1966; **14**:328–36.

24 Monsigny M, Roche AC, Midoux P. Uptake of neoglycoproteins via membrane lectin(s) of L1210 cells evidenced by quantitative flow cytofluorometry and drug targeting. Biol Cell 1984; **51**:187–96.

25 Hnatowich DJ, Layne WW, Childs RL. The preparation and labeling of DTPA-coupled albumin. Int J Appl Radiat Isot 1982; **33**:327–32.

26 Duncan JR, Welch MJ. Intracellular metabolism of indium-111-DTPA-labeled receptor targeted proteins. J Nucl Med 1993; **34**:1728–38.

27 Moore MW, Carbone FR, Bevan MJ. Introduction of soluble protein into the class I pathway of antigen processing and presentation. Cell 1988; **54**:777–85.

28 Yamasaki Y, Sumimoto K, Nishikawa M, Yamashita F, Yamaoka K, Hashida M, Takakura Y. Pharmacokinetic analysis of *in vivo* disposition of succinylated proteins targeted to liver nonparenchymal cells via scavenger receptors: importance of molecular size and negative charge density for in vivo recognition by receptors. J Pharmacol Exp Ther 2002; **301**:467–77.

29 Takahashi K. The structure and function of ribonuclease T1. XXIII. Inactivation of ribonuclease T1 by reversible blocking of amino groups with *cis*-aconitic anhydride and related dicarboxylic acid anhydrides. J Biochem (Tokyo) 1977; **81**:641–6.

30 Kindberg GM, Magnusson S, Berg T, Smedsrod B. Receptor-mediated endocytosis of ovalbumin by two carbohydrate-specific receptors in rat liver cells. The intracellular transport of ovalbumin to lysosomes is faster in liver endothelial cells than in parenchymal cells. Biochem J 1990; **270**:197–203.

31 York IA, Rock KL. Antigen processing and presentation by the class I major histocompatibility complex. Annu Rev Immunol 1996; **14**:369–96.

32 Bonifaz L, Bonnyay D, Mahnke K, Rivera M, Nussenzweig MC, Steinman RM. Efficient targeting of protein antigen to the

dendritic cell receptor DEC-205 in the steady state leads to antigen presentation on major histocompatibility complex class I products and peripheral $CD8^+$ T cell tolerance. J Exp Med 2002; **196**:1627–38.

33 Sallusto F, Cella M, Danieli C, Lanzavecchia A. Dendritic cells use macropinocytosis and the mannose receptor to concentrate macromolecules in the major histocompatibility complex class II compartment. downregulation by cytokines and bacterial products. J Exp Med 1995; **182**:389–400.

34 Fanger NA, Wardwell K, Shen L, Tedder TF, Guyre PM. Type I (CD64) and type II (CD32) Fc gamma receptor-mediated phagocytosis by human blood dendritic cells. J Immunol 1996; **157**:541–8.

35 Rodriguez A, Regnault A, Kleijmeer M, Ricciardi-Castagnoli P, Amigorena S. Selective transport of internalized antigens to the cytosol for MHC class I presentation in dendritic cells. Nat Cell Biol 1999; **1**:362–8.

36 Grant EP, Michalek MT, Goldberg AL, Rock KL. Rate of antigen degradation by the ubiquitin-proteasome pathway influences MHC class I presentation. J Immunol 1995; **155**:3750–8.

37 Jameson SC, Bevan MJ. Dissection of major histocompatibility complex (MHC) and T cell receptor contact residues in a Kb-restricted ovalbumin peptide and an assessment of the predictive power of MHC-binding motifs. Eur J Immunol 1992; **22**:2663–7.

38 Jameson SC, Carbone FR, Bevan MJ. Clone-specific T cell receptor antagonists of major histocompatibility complex class I-restricted cytotoxic T cells. J Exp Med 1993; **177**:1541–50.

39 Yamasaki Y, Hisazumi J, Yamaoka K, Takakura Y. Efficient scavenger receptor-mediated hepatic targeting of proteins by introduction of negative charges on the proteins by aconitylation: the influence of charge density and size of the proteins molecules. Eur J Pharm Sci 2003; **18**:305–12.

Biodistribution Characteristics of Galactosylated Emulsions and Incorporated Probucol for Hepatocyte-Selective Targeting of Lipophilic Drugs in Mice

Emi Ishida,[1] Chittima Managit,[1] Shigeru Kawakami,[1] Makiya Nishikawa,[2] Fumiyoshi Yamashita,[1] and Mitsuru Hashida[1,3]

Received November 11, 2003; accepted March 5, 2004

Purpose. Galactosylated emulsions containing cholesten-5-yloxy-*N*-(4-((1-imino-2-D-thiogalactosylethyl)amino)butly)formamide (Gal-C4-Chol) as a "homing device" were developed for hepatocyte-selective drug targeting. The targeting efficiency of galactosylated emulsions was evaluated by a distribution study in mice.

Methods. Soybean oil/EggPC/cholesterol (Chol) (weight ratio, 70:25:5) (bare) emulsions and soybean oil/EggPC/Gal-C4-Chol (weight ratio, 70:25:5) (Gal) emulsions were prepared and labeled with [^{3}H]cholesteryl hexadecyl ether (CHE). [^{14}C]probucol as a model lipophilic drug was incorporated in the emulsions or EggPC/Chol/Gal-C4-Chol (Gal) liposomes. Their tissue and intrahepatic distribution were evaluated following intravenous injection in mice.

Results. After intravenous injection, Gal-emulsions were rapidly eliminated from the blood and accumulated in the liver, in contrast to the bare-emulsions. The liver uptake clearance of Gal-emulsions was 3.2- and 1.2-times greater than that of bare-emulsions and Gal-liposomes, respectively. The uptake ratio in liver parenchymal cells (PC) and nonparenchymal cells (NPC) of Gal-emulsions was higher than that of Gal-liposomes, being 7.4 and 3.0, suggesting that Gal-emulsions are an effective PC-selective carrier. The hepatic uptake of Gal-emulsions, but not that of bare-emulsions, was significantly inhibited by the pre-dosing of not only lactoferrin but also Gal-liposomes, suggesting asialoglycoprotein receptor-mediated endocytosis. Furthermore, [^{14}C]probucol incorporated in Gal-emulsions was efficiently delivered to the liver compared with Gal-liposomes.

Conclusion. Gal-emulsions have been proven to be an alternative carrier for hepatocyte-selective drug targeting.

KEY WORDS: galactosylated emulsions; hepatocytes; lipophilic drug; targeting.

INTRODUCTION

Receptor-mediated drug targeting is a promising approach to cell-selective drug delivery (1). One particular method exploits the sugar recognition mechanisms that specific cell types possess. Receptors for carbohydrates, such as the asialoglycoprotein receptor on hepatocytes and the mannose receptor on several macrophages and liver endothelial cells, recognize the corresponding sugars on the nonreducing terminal of sugar chains. Recently, we synthesized a novel galactosylated cholesterol derivative, that is, cholesten-5-yloxy-*N*-(4-((1-imino-2-D-thiogalactosylethyl)amino)butyl) formamide (Gal-C4-Chol), to modify liposomes with galactose moieties for hepatocytes drug targeting (2). However, for certain lipophilic drugs, liposomal carrier systems are of limited use for delivery because of their restricted solubilizing capacity. Even though a drug carrier exhibits a favorable *in vivo* disposition profile, limited solubility of the incorporated drugs may lead to failure in achieving sufficient therapeutic efficacy.

Lipid emulsions are considered to be superior to liposomes due to the fact that they can be produced on an industrial scale, are stable during storage, are highly biocompatible, and have a high solubilizing capacity as far as lipophilic drugs are concerned (3,4) because lipid emulsions possess an oil phase in particulate form, so that it can dissolve large amounts of highly lipophilic drugs. In this context, lipid emulsions have widely been used as drug carriers, especially as long-circulating drug carriers for passive targeting (5–7). Cell-specific drug targeting is sometimes urgently required for a variety of clinical purposes; however, there are few reports of cell-specific drug targeting using lipid emulsions. Recently, Rensen *et al.* developed novel apo E–associated emulsions for hepatocytes targeting (8,9). These apo E–associated emulsions are reported to be selectively taken up by liver parenchymal cells and are useful for delivery of antiviral drugs, such as iododeoxyuridine, to hepatocytes. However, introduction of apo E to the carrier is rather complicated, and so there can be problems as far as the reproducibility and stability of apo E emulsions are concerned. The lipid emulsion (oil-in-water) surface exhibits aqueous properties; thus, a galactose moiety could be covered on the emulsion surface when Gal-C4-Chol was added because galactose is a hydrophilic molecule, and so the galactose moiety would be fixed on the emulsions surface.

The purpose of this study was to elucidate the biodistribution characteristics of galactosylated (Gal-) emulsions after intravenous administration as a novel drug carrier to hepatocytes. Then, we examined the applicability of probucol, which is a model lipophilic drug, to investigate the usefulness of the drug carrier. The targeting efficiency of probucol incorporated in emulsions was compared with that in EggPC/Chol/Gal-C4-Chol liposomes, which is the optimized lipid composition for the targeted delivery of probucol by Gal-liposomes (10). [^{3}H]Cholesteryl hexadecyl ether (CHE) was used as an emulsion marker (11).

MATERIALS AND METHODS

Chemicals

N-(4-aminobutyl)carbamic acid *tert*-butyl ester was purchased from Tokyo Chemical Industry (Tokyo, Japan). Cholesteryl chloroformate was obtained from Sigma Chemicals (St. Louis, MO, USA). Egg phosphatidylcholine (EggPC) and soybean oil were purchased from Wako Pure Chemicals Industry Ltd. (Osaka, Japan). Cholesterol (Chol) and Clear-Sol I were purchased from Nacalai Tesque (Kyoto, Japan). Soluene 350 was obtained from Packard (Groningen, The Netherlands). [^{3}H]Cholesteryl hexadecyl ether (CHE) was pur-

[1] Department of Drug Delivery Research, Graduate School of Pharmaceutical Sciences, Kyoto University, Sakyo-ku, Kyoto 606-8501, Japan.

[2] Department of Biopharmaceutics and Drug Metabolism, Graduate School of Pharmaceutical Sciences, Kyoto University, Sakyo-ku, Kyoto 606-8501, Japan.

[3] To whom correspondence should be addressed. (e-mail: hashidam@pharm.kyoto-u.ac.jp)

0724-8741/04/0600-0932/0

chased from NEN Life Science Products Inc. (Boston, MA, USA). [^{14}C]Probucol was purchased from Daiichi Radioisotopes (Tokyo, Japan). All other chemicals were of the highest purity available.

Synthesis of Gal-C4-Chol

Gal-C4-Chol was synthesized by the method described previously (2). Briefly, cholesteryl chloroformate was reacted with *N*-(4-aminobutyl) carbamic acid *tert*-butyl ester in chloroform for 24 h at room temperature and then incubated with trifluoroacetic acid for 4 h at 4°C. *N*-(4-aminobutyl)-(cholesten-5-yloxyl)formamide was obtained after evaporation of the solvent. A quantity of the resultant material was added to an excess of 2-imino-2-methoxyethyl-1-thiogalactoside (12) in pyridine containing triethylamine. After 24 h incubation at room temperature, the reaction mixture was evaporated, resuspended in water, and dialyzed against distilled water for 48 h using a semipermeable membrane (12 kDa cutoff). Finally, the dialyzate was lyophilized.

Preparation of Emulsions and Liposomes

Bare-emulsions consisted of soybean oil, EggPC, and Chol at a weight ratio of 70:25:5. Gal-emulsions contained soybean oil, EggPC, and Gal-C4-Chol at a weight ratio of 70:25:5. Bare-liposomes consisted of EggPC and Chol at a molar ratio of 60:40. Gal-liposomes consisted of EggPC, Chol, and Gal-C4-Chol at a molar ratio of 60:35:5. The lipid mixture was dissolved in chloroform, vacuum-desiccated, and resuspended in 5 ml sterile phosphate-buffered saline (pH 7.4). The suspension was sonicated for 20 min (200 W) under a current of nitrogen. As for liposomes, after hydration, the suspension was sonicated for 3 min (200 W), and the resulting liposomes were passed through 200-nm (5 times) and 100-nm (5 times) polycarbonate membrane filters using an extruder device. The concentration of the emulsions and liposomes was adjusted to 0.5% based on radioactivity measurement so that the total EggPC, Chol, and Gal-C4-Chol content was equivalent to 0.5 g per 100 ml. Radiolabeling of the emulsions and liposomes was performed by addition of [^{3}H]CHE (500 μCi) and/or [^{14}C]probucol (50 μCi) with probucol (13.8 μg) to the lipid mixture before formation of a thin film layer. [^{14}C]Probucol dissolved serum was prepared by addition of mouse serum into a thin film of [^{14}C]probucol (50 μCi) and probucol (13.8 μg). [^{14}C]Probucol dissolved serum was then filtrated through a Mullex HV sterile filter (Millipore, Bedford, USA) before the animal experiments. The particle sizes of the emulsions and liposomes without radioisotope were measured in a dynamic light-scattering spectrophotometer (LS-900, Otsuka Electronics, Osaka, Japan). The zeta potential of emulsions and liposomes without radioisotope was measured electrophoretically using a zeta-potential analyzer (LEZA-500T, Otsuka Electronics). The density of Gal-C4-Chol on emulsions and liposomes was determined by calculating the galactose content of Gal-emulsions and liposomes using the anthrone sulfuric acid method (13).

In vivo Distribution

Five-week-old male ddY mice (25.0–30.0 g) were obtained from Shizuoka Agricultural Co-operative Association for Laboratory Animals (Shizuoka, Japan). All animal experiments were carried out in accordance with the Principles of Laboratory Animal Care as adopted and promulgated by the U.S. National Institutes of Health and the Guideline for Animal Experiments of Kyoto University. [^{3}H]CHE (1.0 μCi/100 μl) and/or [^{14}C]probucol (0.1 μCi/100 μl)-labeled emulsions or liposomes were injected into the tail vein of mice at a dose of 5 mg/kg. In the hepatic uptake inhibition experiments, various compounds were intravenously injected 1 min prior to the intravenous injection of emulsions or liposomes. At given times, blood was collected from the vena cava under anesthesia and mice were then sacrificed. The liver, kidney, spleen, heart, and lung were removed, washed with saline, blotted dry, and weighed. A complete urine collection was obtained by combining the excreted urine and that remaining in the bladder. Ten microliters of blood, 200 μl of urine, and a small amount of each tissue were digested with 0.7 ml Soluene-350 by incubating the samples overnight at 45°C. Following digestion, 0.2 ml isopropanol, 0.2 ml 30% hydroperoxide, 0.1 ml 5 N HCl, and 5.0 ml Clear-Sol I were added. The samples were stored overnight, and the radioactivity was measured using a liquid scintillation counter (LSA-500, Beckman, Tokyo, Japan).

Hepatic Cellular Localization

The separation of liver parenchymal cells and nonparenchymal cells was performed according to collagenase perfusion method (14). Briefly, mice were anesthetized with pentobarbital sodium (40–60 mg/kg) and given an intravenous injection of [^{3}H]CHE (0.5–1.0 μCi/100 μl)-labeled emulsions or liposomes. The body temperatures were kept at 37°C with a heat lamp during the experiment. Then, 30 min after administration, the liver was perfused first with Ca^{2+}, Mg^{2+}-free perfusion buffer [10 mM *N*-2-hydroxyethylpiperazine-*N'*-2-ethanesulfonic acid (HEPES), 137 mM NaCl, 5 mM KCl, 0.5 mM NaH_2PO_4, and 0.4 mM Na_2HPO_4, pH 7.2] for 10 min followed by perfusion buffer supplemented with 5 mM $CaCl_2$ and 0.05% (w/v) collagenase (type I; pH 7.5) for 10 min. As soon as the perfusion started, the vena cava and aorta were cut, and the perfusion rate was maintained at 3–4 ml/min. Following the discontinuation of perfusion, the liver was excised, and its capsular membranes were removed. The cells were dispersed by gentle stirring in ice-cold Hank's-HEPES buffer containing 0.1% BSA. The dispersed cells were filtered through cotton mesh sieves, followed by centrifugation at 50 × *g* for 1 min. The pellets containing parenchymal cells (PC) were washed twice with Hank's-HEPES buffer by centrifuging at 50 × *g* for 1 min. The supernatant containing nonparenchymal cells (NPC) was similarly centrifuged twice. The resulting supernatant was then centrifuged twice at 200 × *g* for 2 min. PC and NPC were resuspended separately in ice-cold Hank's-HEPES buffer (4 ml for PC and 1.8 ml for NPC). The cell numbers and viability were determined by the trypan blue exclusion method. Then, the radioactivity in the cells (0.5 ml) was determined as for the other tissue samples.

Calculation of Organ Clearance

Tissue distribution data were evaluated using the organ distribution clearances as reported previously (15). Briefly, the tissue uptake rate can be described by the following equation:

$$\frac{dX_t}{dt} = CL_{uptake} \cdot C_b \quad (1)$$

where X_t is the amount of [^{3}H]-labeled emulsions or liposomes in the tissue at time t, CL_{uptake} is the tissue uptake clearance, and C_b is the blood concentration of [^{3}H]-labeled emulsions or liposomes. Integration of Eq. (1) gives

$$X_t = CL_{uptake} \cdot AUC_{(0-t)} \quad (2)$$

where $AUC_{(0-t)}$ represents the area under the blood concentration-time curve from time 0 to t. The CL_{uptake} value can be obtained from the initial slope of a plot of the amount of [^{3}H]-labeled emulsions or liposomes in the tissue at time t (X_t) vs. the area under the blood concentration-time curve from time 0 to t [$AUC_{(0-t)}$].

Statistical Analysis

Statistical comparisons were performed using Student's unpaired t test. $p < 0.05$ was considered to be indicative of statistical significance.

RESULTS

Physicochemical Properties of Emulsions

Sinusoids in the liver lobules have a unique type of endothelial lining consisting of endothelial cells with flattened processes perforated by small fenestrae about 100 nm in size (16). Therefore, emulsions and liposomes with a diameter less than this can readily pass through the fenestration into the Disse space. Accordingly, we prepared emulsions and liposomes less than 100 nm in diameter in order to allow free access to hepatocytes.

Table I summarizes the lipid composition, particle sizes, and zeta potential of the emulsions and liposomes prepared. These emulsions and liposomes were very similar in size with a mean diameter of approximately 100 nm. As shown by the zeta potential, the surface charge of each particle was almost neutral. In addition, the particle size and zeta potential of the emulsions and liposomes were kept constant for a period of at least 2 months at 4°C (data not shown).

Biodistribution of [^{3}H]-Labeled Emulsions

[^{3}H]CHE was selected as a tracer of emulsion (11,17) and liposomes (10,11). Figures 1 and 2 show the blood concentration-, tissue accumulation-, and urine excretion-time course of [^{3}H]-labeled soybean oil/EggPC/Chol (70:25:5) (bare) emulsions, soybean oil/EggPC/Gal-C4-Chol (70:25:5) (Gal) emulsions, EggPC/Chol (60:40) (bare) liposomes, and EggPC/Chol/Gal-C4-Chol (60:35:5) (Gal) liposomes after intravenous injection. In contrast to the bare-emulsions, Gal-emulsions were rapidly eliminated from the blood circulation and mostly recovered in the liver, accounting for 75% of the dose, within 30 min. Gal-liposomes, which have the same Gal-C4-Chol density as that of Gal-emulsions, were also rapidly eliminated from the blood circulation and mostly recovered in the liver, accounting for 60% of the dose, within 30 min.

Pharmacokinetic Analysis of Biodistribution of [^{3}H]-Labeled Emulsions

To compare the disposition profiles of emulsions and liposomes, initial distribution in the early phase up to 10 min, in which the contribution of metabolites can be ignored, was quantified using tissue uptake clearances parameter.

Table II summarizes the area under blood concentration-time curve (AUC) and tissue uptake clearances calculated for the initial 10 min for liver (CL_{liver}), kidney (CL_{kidney}), spleen (CL_{spleen}), lung (CL_{lung}), heart (CL_{heart}), and urine (CL_{urine}) of the [^{3}H]-labeled emulsions and liposomes. The AUC of Gal-emulsions was much lower than that of bare-emulsions. The liver uptake clearance of Gal-emulsions was 3.2-times greater than that of bare-emulsions. Also, the liver uptake clearance of Gal-emulsions was 1.2-times higher than that of Gal-liposomes.

Effect of Gal-C4-Chol Content of Emulsions on Hepatic Accumulation

The amounts of [^{3}H]-labeled emulsions recovered in the liver at 30 min after intravenous injection of Gal-emulsions containing various amounts of Gal-C4-Chol was evaluated. The density of Gal-C4-Chol in the emulsions was calculated to be 3.0×10^{12}, 8.9×10^{12}, and 1.5×10^{13}/unit surface area (cm^2) for Gal-emulsions containing, respectively, a 1%, 3%, and 5% weight ratio of Gal-C4-Chol. All emulsions prepared have almost similar particle sizes (data not shown). As shown in Fig. 3, the liver accumulation of Gal-emulsions increased with the amount of Gal-C4-Chol in the emulsions. The relationship between the liver accumulation and the galactose density of the emulsions on the emulsions surface correlates well, suggesting that the galactose density on the surface of the emulsions is important as far as recognition by the asialoglycoprotein receptors on hepatocytes is concerned.

Table I. Lipid Composition, Mean Diameter, and Zeta Potential of the Tested Emulsions and Liposomes

Formulations	Lipid composition	Mean diameter[a] (nm)	Zeta potential[b] (mV)
Bare-emulsions	Soybean oil:EggPC:Chol (70:25:5) (weight ratio)	100.0 ± 2.3	4.0 ± 1.4
Gal-emulsions	Soybean oil:EggPC:Gal-C4-Chol (70:25:5) (weight ratio)	104.5 ± 3.8	4.7 ± 0.5
Bare-liposomes	EggPC:Chol (60:40) (molar ratio)	93.3 ± 11.2	4.4 ± 0.2
Gal-liposomes	EggPC:Chol:Gal-C4-Chol (60:35:5) (molar ratio)	96.2 ± 5.8	9.0 ± 1.7

EggPC, egg phosphatidylcholine; Chol, cholesterol.

[a] Diameter of emulsions and liposomes was measured by dynamic light-scattering spectrophotometry. Results are expressed as the mean ± SD of three experiments.

[b] Zeta potential of emulsions and liposomes was measured by electrophoretic light-scattering spectrophotometry. Results are expressed as the mean ± SD of three experiments.

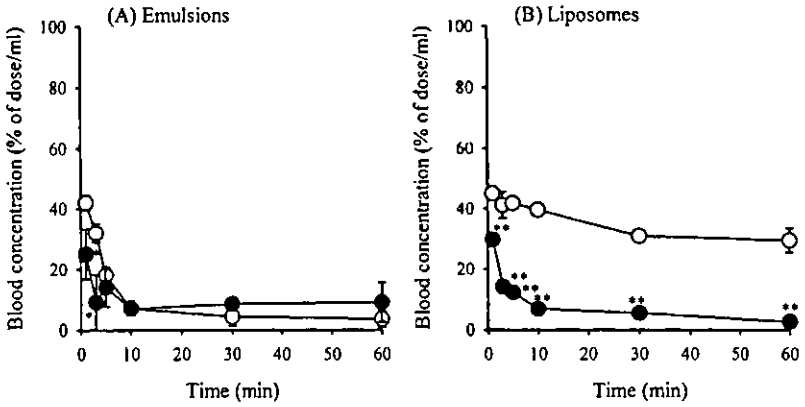

Fig. 1. Blood concentration of [^{3}H]-labeled (A) bare-(○) and Gal-(●) emulsions and (B) bare-(○) and Gal-(●) liposomes after intravenous injection into mice. Each value represents the mean ± SD of three experiments. Statistically significant differences (*$p < 0.05$, **$p < 0.01$) from control group.

Hepatic Cellular Localization of [^{3}H]-Labeled Emulsions

Figure 4 shows the hepatic cellular localization of [^{3}H]-labeled emulsions and liposomes 30 min after intravenous injection. Compared with bare-emulsions, Gal-emulsions accumulated selectively in PC with a PC/NPC ratio of 7.4. Moreover, Gal-liposomes also accumulated selectively in PC with a PC/NPC ratio of 3.0. Thus, the PC selectivity of the Gal-emulsions is higher than that of Gal-liposomes.

Inhibition of Hepatic Uptake of Emulsions by Pre-dosing Various Agents

Figure 5 shows the effect of pre-dosing with various agents on the hepatic accumulation of [^{3}H]-labeled bare- and Gal-emulsions. The liver uptake of Gal-emulsions was significantly inhibited by pre-dosing lactoferrin, which is a ligand of chylomicron remnant receptors on liver parenchymal cells, and Gal-liposomes, which contain a ligand for asialoglycopro-

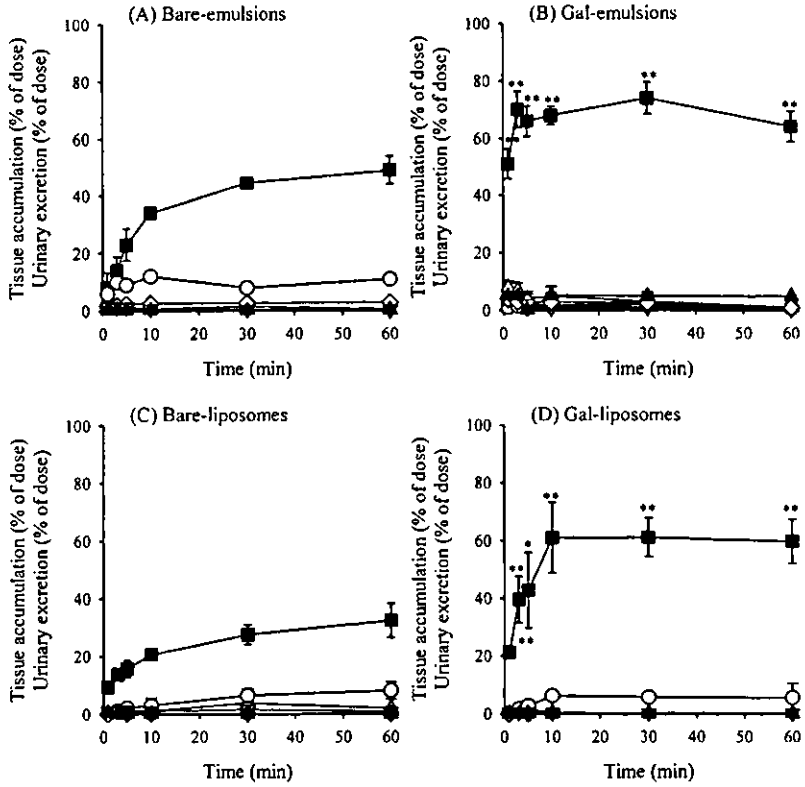

Fig. 2. Tissue accumulation of [^{3}H]-labeled (A) bare-emulsion, (B) Gal-emulsion, (C) bare-liposomes, and (D) Gal-liposomes after intravenous administration into mice. Radioactivity was determined in the liver (■), kidney (△), spleen (○), lung (▽), heart (◇), and urine (▲). Each value represents the mean ± SD of three experiments. Statistically significant differences (*$p < 0.05$, **$p < 0.01$) from each bare emulsion (A vs. B) or bare liposomes (C vs. D).

Table II. Area Under the Blood Concentration-Time Curve (AUC) and Tissue Uptake Clearance of [^{3}H]-Labeled Emulsions and Liposomes After Intravenous Injection Into Mice[a]

Formulations	AUC (% of dose × h/ml)	Clearance[a] (μl/h)					
		CL_{liver}	CL_{kidney}	CL_{spleen}	CL_{lung}	CL_{heart}	CL_{urine}
Bare-emulsions	3.7	9480	201	570	179	31	3
Gal-emulsions	1.9	31,200	1350	1040	239	705	1360
Bare-liposomes	7.0	2960	121	407	152	102	6
Gal-liposomes	2.4	25,300	313	2610	129	76	67

[a] AUC and clearance (CL) were calculated for the period until 10 min after injection. An average of three experiments is shown.

tein receptors on liver parenchymal cells, whereas no inhibition was observed in the case of bare-emulsions.

Blood Elimination and Hepatic Accumulation of [^{14}C]Probucol Incorporated into [^{3}H]-Labeled Gal-Emulsions and Gal-Liposomes

Figure 6 shows the blood concentration and liver accumulation of [^{14}C]probucol dissolved in serum, which represents the original distribution of probucol, [^{14}C]probucol incorporated into [^{3}H]-labeled Gal-emulsions and Gal-liposomes after intravenous injection. [^{14}C]Probucol was dissolved in serum to analyze the inherent distribution of probucol to investigate the controlled distribution of probucol by Gal emulsions and liposomes. Rapid blood elimination of [^{14}C]probucol was observed in Gal-emulsions, followed by Gal-liposomes. Similarly, the fastest blood elimination of [^{3}H]CHE was observed in Gal-emulsions, followed by Gal-liposomes. As for the liver accumulation, rapid liver uptake of [^{14}C]probucol was observed in Gal-emulsions followed by Gal-liposomes. Similarly, the highest hepatic uptake of [^{3}H]CHE was observed in Gal-emulsions, followed by Gal-liposomes.

The Uptake Clearance of [^{14}C]Probucol Incorporated into [^{3}H]-Labeled Gal-Emulsions and Gal-Liposomes

Table III summarizes the AUC and tissue uptake clearances of [^{14}C]probucol incorporated into [^{3}H]-labeled Gal-emulsions and Gal-liposomes. The lowest AUC was observed in Gal-emulsions followed by Gal-liposomes. The liver uptake clearance of [^{14}C]probucol incorporated into [^{3}H]-labeled Gal-emulsions was 1.6-times higher than that into Gal-liposomes.

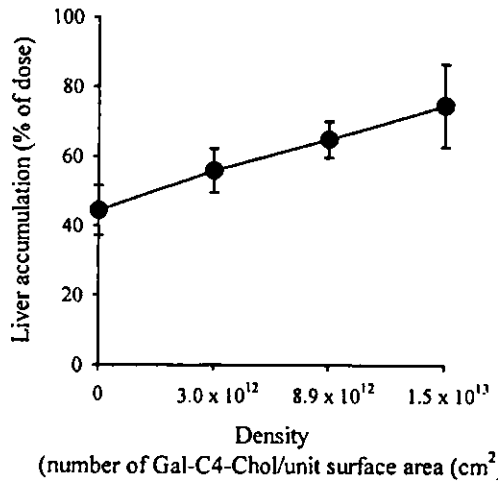

Fig. 3. Liver accumulation of [^{3}H]-labeled Gal-emulsions 30 min after intravenous administration into mice. Gal-emulsions were prepared with various amounts of Gal-C4-Chol. Each value represents the mean ± SD of three experiments.

DISCUSSION

This manuscript summarizes our initial efforts to investigate whether Gal-emulsions would offer a significant advantage as an alternative carrier for drug targeting to hepatocytes. Several investigators have demonstrated that the liposomes that were modified with native glycoproteins (18,19) or synthetic glycolipids possessing tris-galactosides (20) were efficiently recognized by asialoglycoprotein receptors. However, there are several potential problems in using these compounds due to their complicated structures, difficulty in achieving industrial-scale production, and possible antigenicity. Recently, we synthesized Gal-C4-Chol having bifunctional properties of a lipophilic anchor moiety for stable incorporation into liposomes and a galactose moiety for recognition by the asialoglycoprotein receptors (21). Our strategy for efficient targeting of liposomes by glycosylation is to achieve stable fixation of the sugar moiety on the surface of the liposomes under *in vivo* conditions. Therefore, cholesterol was chosen as a hydrophobic anchor, which is stably associated with the liposomal membrane (22,23), and only monogalactoside was introduced to the lipid as a ligand because introduction of many hydrophilic galactose moieties to a lipid anchor would result in their removal from liposomes by interaction with lipoproteins and/or other lipid compartments under *in vivo* conditions (20). In fact, we found that eggPC or

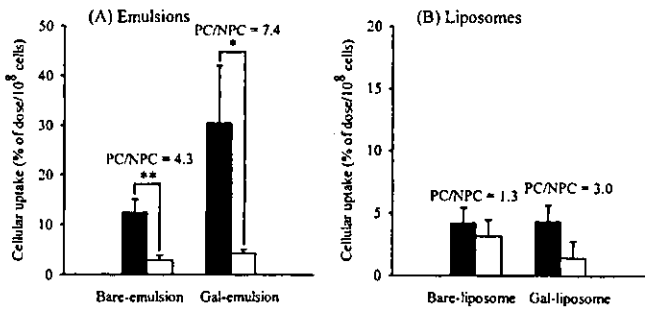

Fig. 4. Hepatic cellular localization of (A) [^{3}H]-labeled emulsions and (B) [^{3}H]-labeled liposomes after intravenous administration into mice. Radioactivity was determined 30 min postinjection in PC (■), and NPC (□). Each value represents the mean + SD of three experiments. Statistically significant differences (*$p < 0.05$, **$p < 0.01$) from control group.

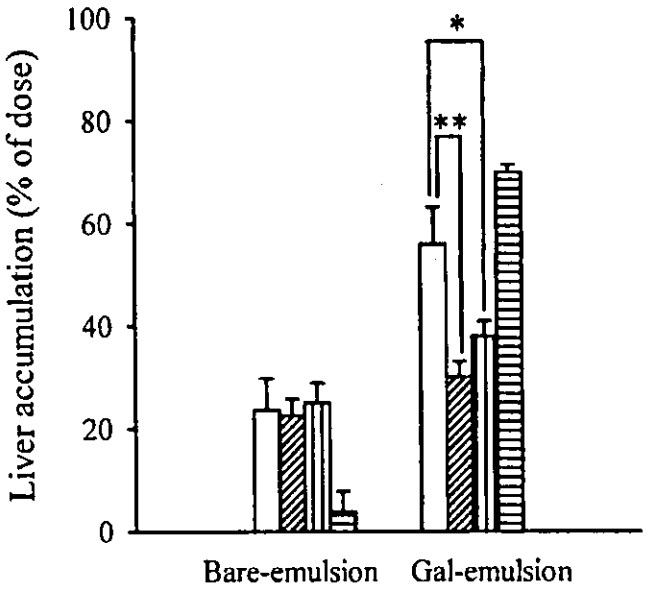

Fig. 5. Inhibition of liver uptake of [^{3}H]-labeled emulsions after intravenous preinjection of various compounds. Liver accumulation was determined at 5 min. Emulsions were injected without (□) or with preinjection of lactoferrin (▨), Gal-liposomes (▥), or an excess of bare-emulsions (▤). Each value represents the mean + SD of three experiments. Statistically significant differences (*$p < 0.05$, **$p < 0.01$) from control group.

DSPC/Chol/Gal-C4-Chol (Gal-) liposomes were rapidly taken up by hepatocytes via asialoglycoprotein receptor–mediated endocytosis (10,21). Thus, the Gal-C4-Chol combination with soybean oil, EggPC, and Chol gave emulsion formulations with suitable pharmaceutical characteristics for targeting under *in vivo* conditions.

As shown in Figs. 2 and 4, [^{3}H]-labeled Gal-emulsions exhibited marked hepatic uptake and rather high PC/NPC ratios, suggesting that Gal-emulsions were more efficiently taken up into hepatocytes compared with bare-emulsions. To investigate the uptake mechanism of Gal-emulsions, we performed a competitive inhibition experiment involving predosing lactoferrin, Gal-liposomes, and bare-emulsions (Fig. 5). Pre-dosing lactoferrin, which is a ligand of chylomicron remnant receptors on liver parenchymal cells (24), significantly inhibited the liver uptake of Gal-emulsions. It has also been reported that lactoferrin can bind to asialoglycoprotein receptors on liver parenchymal cells (24,25); therefore, this result does not make it clear whether the uptake of Gal-emulsions involves chylomicron remnant receptor– or asialoglycoprotein receptor–mediated endocytosis. However, the liver uptake of Gal-emulsions was also markedly inhibited by Gal-liposomes, which contain a ligand of asialoglycoprotein receptors (10), but was not inhibited by bare-emulsions (Fig. 5). Taking these findings into consideration, this suggests that Gal-emulsions were taken up by asialoglycoprotein-mediated endocytosis after intravenous administration.

We have established methods for introducing galactose moieties directly into various molecular species and developed various macromolecular drug carrier systems (26,27), protein derivatives (28,29), and liposomes (30–33) that show superior liver targeting via asialoglycoprotein receptor–mediated endocytosis. As far as the molecular design of the galactosylated protein is concerned, we have demonstrated that the recognition of galactosylated protein by the liver cells is based on the estimated surface density of the galactose residues (34). In this study, we showed that the galactose density on the surface of the Gal-emulsions is an important factor for recognition by the asialoglycoprotein receptors on hepatocytes, suggesting that enhancing the recognition by asialoglycoprotein receptors can be controlled by the amount of added Gal-C4-Chol. This observation correlates well with the effect of the galactose density of galactosylated liposomes, which possess a mono-galactoside, that have been studied by Murahashi *et al.* (35).

In order to achieve drug targeting by a cell-selective approach, the drug release properties from emulsions are important for drug targeting, and so we investigated the relationship between the movement of Gal-emulsions and incorporated probucol. We previously investigated the *in vivo* disposition of drugs with a variety of lipophilicities, incorporated into liposomes, lipid emulsions, and micelles, based on

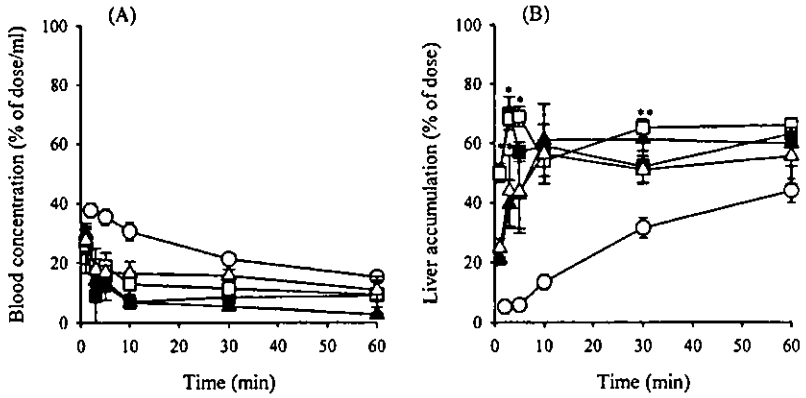

Fig. 6. (A) Blood concentration and (B) liver accumulation of [^{14}C]-labeled probucol dissolved in serum (○) or [^{3}H]CHE-labeled Gal-emulsions (■) and [^{3}H]CHE-labeled Gal-liposomes (▲) or [^{14}C]-labeled probucol incorporated Gal-emulsions (□) and [^{14}C]-labeled probucol incorporated Gal-liposomes (△) after intravenous administration into mice. Each value represents the mean ± SD of three experiments. Statistically significant differences (*$p < 0.05$, **$p < 0.01$) between Gal-emulsions and Gal-liposomes.